Thesis for the degree of Doctor of Philosophy

Advanced and Autonomous Applications of Optical Tweezers

Martin Selin

Department of Physics
University of Gothenburg

Göteborg, Sweden 2025

UNIVERSITY OF GOTHENBURG

Advanced and Autonomous Applications of Optical Tweezers

Martin Selin
ISBN: 978-91-8115-409-2 (*Printed version*)
ISBN: 978-91-8115-410-8 (*PDF*)
Available at http://hdl.handle.net/2077/87446

Department of Physics
University of Gothenburg, SE-412 96 Göteborg
Tel: +46 (0)31-7721000, Fax: +46 (0)31-7723496
http://www.physics.gu.se

Printed by STEMA SPECIALTRICK AB
Göteborg, Sweden 2025

Progress in science depends on new techniques, new discoveries, and new ideas, probably in that order.

Sydney Brenner (1927-2019)

Contents

Sammanfattning

Uppfinnandet av mikroskopet i slutet av 1500-talet avslöjade en tidigare dold mikroskopisk värld och gjorde det möjligt att direkt observera strukturer och organismer bortom gränsen för människans synförmåga. Sedan dess har betydelsen av denna värld för människors hälsa, materialvetenskap och avancerad teknik drivit utvecklingen av alltmer sofistikerade analysmetoder. Av dessa har optiska pincetter blivit ett centralt verktyg. De använder lasrar för att manipulera och undersöka objekt med hög precision, vilket möjliggör studier av enskilda molekyler, celler och partiklar.

De senaste åren har intresset för artificiell intelligens (AI) driven av maskininlärning ökat kraftigt och används nu brett inom forskning. I artikel I undersöker vi hur dessa metoder kombinerats med optiska pincetter och hur denna kombination kan komma att utvecklas samt ger riktlinjer för hur de kan användas. Artikel II presenterar en optisk pincett som kan utföra experiment helt autonomt. För detta har särskild elektronik, mjukvara och automationsalgoritmer utvecklats. Med detta system genomförde vi fyra representativa experiment och kunde därigenom visa både reproducerbarhet och möjligheten till helt automatiserad drift. I artikel III användes den optiska pincetten för att studera adsorption och desorption av partiklar vid gränsytan mellan två vätskor, vilket avslöjade tidigare okänd dynamik. Slutligen behandlar artikel IV utmaningarna med kalibrering under icke ideala förhållanden, specifikt fallen med låg samplingsfrekvens och långa integrationstider. Vidare presenterar vi ett ramverk för att hantera i mätningar under sådana förhållanden.

Tillsammans introducerar dessa arbeten flera nya tekniker för optiska pincetter, från kolloidstudier till automation och kalibrering. Särskilt automationen kommer att vara viktigt för utvecklingen av optiska pincetter genom att knyta samman mätningar av enstaka molekyler med ensemblemätningar. Detta kan möjliggöra användningen av AI för modellering och användandet av optiska pincetter för storskaliga datadrivna studier.

Abstract

The invention of the microscope in the late 16th century revealed a hidden microscopic world, allowing direct observation of structures and organisms beyond the limit of human vision. Since then, the importance of this world for human health, materials science, and advanced technology has driven the development of increasingly sophisticated analysis methods. Among these, optical tweezers have become a central tool, using lasers to manipulate and probe objects with exceptional precision enabling single-molecule, single-cell, and single-particle studies.

Recent years have seen explosive growth in the use of artificial intelligence (AI), particularly machine learning, across research. In Paper I, we examine how these methods are used in optical tweezers and the likely trajectory of their integration and give some guidelines. Paper II presents an optical tweezers system with custom electronics, firmware, user interface which together makes the instrument capable of performing experiments fully autonomously. Using this system, we performed four representative experiments, demonstrating both reproducibility and variety of autonomous experiments. In Paper III, the system was applied to probe particle adsorption and desorption at liquid–liquid interfaces, revealing previously unseen dynamics of these processes. Finally, Paper IV addresses the challenge of force calibration under non-ideal conditions, in particular low sampling rates and long integration times, and proposes a framework to handle these challenges.

Together, these works introduce several new techniques for optical tweezers, spanning colloidal studies, automation, and trajectory analysis. Automation in particular will be crucial for the future of optical tweezers by bridging the gap between single-molecule, cell or particle studies and ensemble measurements, enabling the application of deep learning for advanced modeling and unlocking the potential of optical tweezers for large, data-driven studies.

This thesis is based on the work contained in the following scientific papers:

Paper I: Deep learning for optical tweezers.
Antonio Ciarlo, David Bronte Ciriza, **Martin Selin**, Onofrio M. Maragò, Antonio Sasso, Giuseppe Pesce , Giovanni Volpe and Mattias Goksör
Nanophotonics 2024, 13.17: 3017-3035.

Paper II: SmartTrap: Automated Precision Experiments with Optical Tweezers.
Martin Selin, Antonio Ciarlo, Giuseppe Pesce, Lars Bengtsson, Joan Camunas-Soler, Vinoth Sundar Rajan, Fredrik Westerlund, L. Marcus Wilhelmsson, Isabel Pastor, Felix Ritort, Steven B. Smith, Carlos Bustamante, and Giovanni Volpe
arXiv preprint arXiv:2505.05290 (2025), submitted June 2025

Paper III: Dynamics of core-shell particles absorbing and desorption into liquid-liquid interfaces.
Martin Selin, Maret Ickler, Gerardo Campos-Villalobos, Fabrizio Camerin, Nicolas Vogel, Antonio Ciarlo, Giovanni Volpe and Marcel Rey
Manuscript in preparation.

Paper IV: Optimal calibration of optical tweezers with arbitrary integration time and sampling frequencies: a general framework.
Laura Pérez-García, **Martin Selin**, Antonio Ciarlo, Alessandro Magazzù, Giuseppe Pesce, Antonio Sasso, Giovanni Volpe, Isaac Pérez Castillo, and Alejandro V. Arzola
Biomedical Optics Express 14.12 (2023): 6442-6469.

My contributions

Paper I - Deep learning for optical tweezers

Antonio, David and I together came up with the idea for the paper and created the outline of it deciding on what figures to include and how to present these. We all contributed to finding references and in writing and refining the paper. I made my biggest contribution in the writing of the guidelines, where my practical experience with automation proved especially valuable.

Paper II - SmartTrap: Automated Precision Experiments with Optical Tweezers

The SmartTrap paper represents the main work of this thesis. This was initially intended to be (at least) two papers, one describing the updated system and another one describing how this was used to perform DNA pulling experiments autonomously. However, we came to the conclusion that it would likely have a greater impact as a single paper and added three more autonomous experiments, beyond DNA pulling.

I was in charge of most of the different parts of the project, but I received valuable help from the many co-authors along the way. I assembled and tested the instrument, using the old electronics to control it, together with Giuseppe Pesce and Antonio Ciarlo. Throughout, I also made minor changes to the optics and mechanical design to correct for errors by the mechanics workshop and implement improved usability (e.g. motorized the movement of the objective and updated illumination). I also designed the electronics controller, going through more than a dozen revisions of the various circuit boards, Lars Bengtsson taught me how to design circuit boards and how to interface different components (analog-digital-converters,

digital-analog-converters, servomotors, etc.). He also helped me in finding errors in early designs. I wrote all the software, including the firmware for the controller, the complete graphical user interface (GUI), communication protocols, and the automation algorithms. Furthermore I, or rather the instrument I had programmed, conducted the experiments on samples I had prepared. Isabelle Pastor in Felix Ritorts group, and Vinoth were instrumental in teaching me how to perform experiments manually. This included preparing DNA particles and performing experiments. Steven B Smith provided guidance on how to assemble the instrument and provided the DNA used in the final experiments. Carlos, Giovanni, and Joan played a key role in structuring the manuscript and in deciding how to present the results. Lastly, I was also in charge of writing the draft for the paper and preparing figures, including making a full 3D model of the system in Blender for visualization purposes.

Paper III - Dynamics of core-shell particles absorbing and desorption into liquid-liquid interfaces

In this project, I was responsible for the optical tweezers experiments. This included conducting the measurements and designing the experimental protocols. I optimized the microfluidic chamber design to increase the likelihood of forming oil bubbles within the desired size range (approximately 10–20µm in diameter). Additionally, I developed custom procedures to approach oil bubbles in a controlled manner and to carry out particle–particle interaction measurements.

I also handled the data analysis, which involved particle tracking to reconstruct adsorption trajectories and identifying the precise points of adsorption. I prepared the figures for the manuscript and wrote the majority of the initial full draft, excluding the sections on simulations and particle synthesis methods. Along the way I received very valuable input from Maret on the introduction and feedback on the overall draft and Marcel was instrumental in refining the manuscript.

Paper IV: Optimal calibration of optical tweezers with arbitrary integration time and sampling frequencies: a general framework

In this project my biggest contribution was in helping to identify the problem of optical tweezers calibration with long integration times. I had been doing experiments on the correlation of the movement particles optically trapped in holographic tweezers in which I could not use powerful illumination and noticed that the particles were moving less than expected

in the trap (it appeared stiffer than expected). When discussing the issues with these experiments we realized that this problem was largely unexplored. I also did some of the early literature research to verify that this issue had not been addressed on a theoretical level previously, as well as some of the early experiments. Lastly, I assisted in finalizing the manuscript.

Papers not included in this PhD Thesis

Paper V: Influence of sensorial delay on clustering and swarming

Rafal Piwowarczyk, **Martin Selin**, Thomas Ihle, and Giovanni Volpe Physical Review E 100.1 (2019): 012607.

Chapter 1

Optical Tweezers

1.1 Introduction

For dealing with objects in everyday life, we humans have wonderful and versatile tools in the form of our hands [1, 2]. With them, we can pick up and manipulate nearly everything we use day to day. However, for very small (or very large objects which are not relevant for my thesis) objects, different tools are required. In particular, for objects in the micron size range and below, mechanical manipulation is extremely difficult. Such small things may stick to the actuator, break under slight force, or evade capture altogether. Yet, as Richard Feynman famously put it in his now legendary lecture "There is Plenty of Room at the Bottom," there is great value in understanding and controlling the microscopic world: "It is a staggeringly small world that is below... and there is no question that there is enough room on the head of a pin to put all of the Encyclopaedia Britannica." Despite the challenges, exploring this realm is essential for understanding nature. This is especially true in biophysics, where the micro and nanoscales are the domains of cells, biomolecules, the machinery of life itself [3, 4].

This is where optical tweezers come in, offering a non-contact way to manipulate and study objects at the micro and nanoscales [5]. In the most general terms, an optical tweezers is a focused laser beam used to manipulate objects. However, with them you can not only manipulate objects but also measure forces and torques. This has given optical tweezers a wide range of different applications from colloidal chemistry and statistical physics to single-molecule studies and cell sorting [6, 7]. Optical tweezers have proved particularly useful in molecular biology, helping to uncover processes such

as the dynamics of DNA and protein folding as well as the actions of motor proteins [8,9]. Their many applications to biological systems are why Arthur Ashkin was awarded the Nobel prize in 2018 [10].

The use of optical tweezers can be broadly split into different trapping regimes based on the size of objects the objects being trapped and whether trapping is in viscous and non-viscous media [6]. In terms of size ranges, one often discusses three different ones depending on the size of the trapped object relative to the wavelength; these are when the particle is much smaller than the wavelength, about the same size, and much larger than the wavelength. The media can be broadly divided into trapping in air(or vacuum) and viscous media e.g. water.

The focus of this thesis is on trapping in viscous media of particles significantly larger than the wavelength of the trapping laser. In this regime, known as the ray optics regime, it is relatively easy to achieve stable trapping. As discussed in chapter 2, there are many applications within biology and colloidal sciences, not least the aforementioned single-molecule studies which are performed in this regime. This is why it is perhaps the most widely used and studied regime. Still, also when working with large particles in viscous media there are several experimental challenges that need to be overcome. One often needs careful control of the optical trap and high precision position tracking, and, on top of this, additional measurements are often coupled to the tweezers, such as fluorescence.

This contributes to making many optical tweezers experiments highly labor intensive. Not only do you, as operator, need to prepare your samples carefully, but you also need to operate the tweezers itself. Trap particles, move them, and execute advanced measurement protocols. This greatly limits throughput and has limited optical tweezers to applications in research. This may be starting to change with the advent of deep learning in optical tweezers as presented in Paper I and the introduction of advanced automation methods for various experiments presented in Paper II. The applications of optical tweezers are broad, and as we see in Paper III applying the methods to new areas can yield unexpected new insights. Still, some challenges remain. However, as research progresses, more and more problems are solved and new ones appear, the particular problem of long integration times was tackled systematically in Paper IV and now accurate force calibration is straightforward also in these challenging conditions.

1.2 The principles of optical trapping

The idea that light can exert force goes back to Johannes Kepler who in 1619 noted that the tails of comets always point away from the sun. Later, with the help of Maxwell and Poynting, we got a physical explanation to the phenomenon of radiation pressure [11,12]. However, it was not until the invention of lasers that we started to see widespread application of light as a direct source of forces. Central to this development, and that of optical tweezers, was Arthur Ashkin. The experiments he conducted in the early 1970s demonstrated that light can be used to push and trap colloidal particles against a surface [13]. Later he showed that by focusing the laser in the sample it is possible to also trap particles in 3D and the first optical tweezers was created [14].

In its simplest form, an optical tweezers is constructed by focusing a laser beam through a microscope objective into a liquid sample, creating a tightly focused optical trap [5,14]. The fundamental principle behind optical trapping in the ray optics regime is that light carries momentum, which can exert mechanical forces on microscopic objects when the momentum of the light changes due to interaction with these objects through refraction, reflection, or scattering [15].

Objects located near the focus of the laser beam experience optical forces, predominantly what is called the scattering force, F_s, and the gradient force, F_g. The scattering force results primarily from photons scattered by the trapped object. It is directed along the propagation axis of the laser beam, generally pushing the particle away from the focus and potentially preventing stable trapping [16].

The gradient force, on the other hand, is generated by changes in the laser beam's momentum due to refraction at the interface between the trapped particle and the surrounding medium. There are two primary scattering events for the laser beam as it passes through the trapped particle, one when entering and one when exiting, as illustrated by the beams in fig. 1.1. For a focused beam, these will deflect lasers in a direction opposite to the particle's displacement relative to the laser focus. By momentum conservation, the particle experiences an equal but opposite change in momentum, causing it to be pushed towards the laser focus.

For an optical trap to be stable, the gradient force must exceed the scattering force. For a standard optical trap, this requires that the refractive index of the particle is greater than that of the surrounding medium [6,14]. However, using beam-shaping, this requirement can be relaxed [6]. Other optical forces, such as spin-curl forces arising from light polarization and

angular momentum, also exist, but are negligible in most optical trapping scenarios [6]. Besides these optical forces, there are also Brownian forces due to fluid molecules hitting the trapped particle and viscous forces caused by fluid flows.

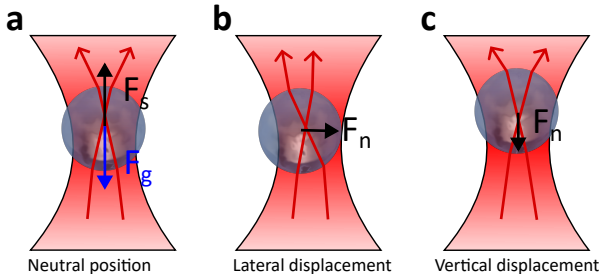

Figure 1.1: **Optically trapped particles and optical forces. a** In a neutral position the scattering and gradient forces, F_s and F_g are equal but in opposite directions. The net force from the trap on the particle is then, $F_n = F_s + F_G$, from the trap on the particle is 0. **b** When the particle is displaced in a lateral direction F_n will be directed towards the trap center. **c** Vertical displacement along the propagation axis will affect how much the laser diverge after passing through the trapped particle also creating a restoring force aimed towards the trap center.

In a first approximation, the optical potential experienced by a trapped spherical particle is harmonic, which makes the optical force linear with the displacement. This means that there is a proportionality constant K relating the displacement Δx to the force F:

$$F \approx -K\Delta x \tag{1.1}$$

The proportionality constant K is referred to as the trap stiffness and it may differ along the different axes. K is particle dependent; in general, a larger refractive index difference between the particle and its surrounding medium results in greater stiffness, while smaller particles also yield higher stiffness [6]. The linear approximation of eq. (1.1) holds well for small deviations from the optical trap center. The process of finding the optical trap stiffness is the subject of calibration discussed in section 1.4.

1.3 Optical tweezers instruments

Today, there are many variations of optical tweezers instruments tailored to different applications and they are often constructed by the laboratory that uses them. Despite the diversity, optical tweezers share key components, most notably a laser and a high numerical aperture focusing objective [5,16]. The laser is sent through the back aperture of the objective to create a tight focus. Because optical tweezers share many components with conventional microscopes, tweezers setups are commonly adapted directly from microscope platforms. A simple optical tweezers design is shown in fig. 1.2. This basic design can be seen as a blueprint upon which more sophisticated setups are built, adding additional functionality.

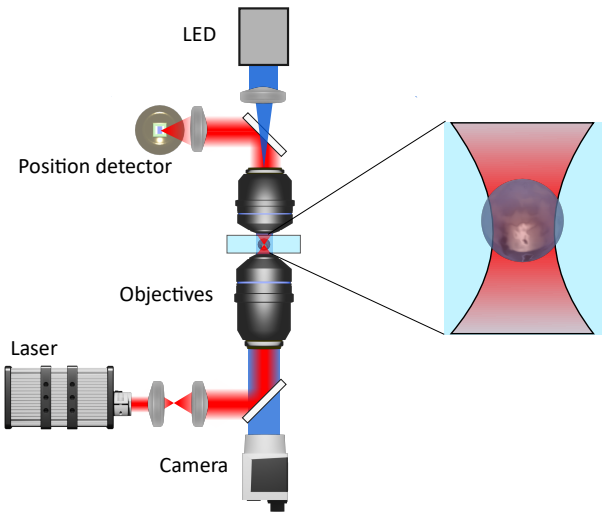

Figure 1.2: **A typical optical tweezers system.** A laser beam (red) is expanded using two lenses and then sent into the optical path of a microscope from the bottom using a dichroic mirror. The objective focuses the beam inside the sample as shown in the inset. After passing through the sample the laser is again collimated by the top objective and then focused onto a photodetector (often a quadrant photodiode, QPD), which is used to monitor the movement of the trapping laser caused by the trapped object. Imaging of the sample is done using standard brightfield configuration (blue beam).

To achieve a stable optical trap, precise beam shaping is essential before the laser enters the objective. In a standard single-trap configuration, this typically involves expanding and collimating the laser beam to overfill the back aperture of the objective. Overfilling ensures that the peripheral rays of the laser contribute to the tight focal spot necessary for efficient trapping. Using a counterpropagating configuration, the overfilling condition may be relaxed as discussed in Section 3.2. This beam expansion is commonly achieved using a telescope configuration consisting of two lenses, as depicted in fig. 1.2 [5]. Advanced beam shaping methods, such as spatial light modulators or adaptive optics, can also be used to overcome specific challenges or to enhance trap stiffness in challenging situations [6, 17].

Lasers used in optical tweezers are typically continuous wave (CW) and operate in the near-infrared region, with a wavelength of 1064 nm being particularly common [5, 16]. This choice is practical because such lasers are widely available and heating effects are limited in water (the most common trapping media) and for both polystyrene and silica particles because of low adsorption. Selecting the appropriate wavelength is crucial to reduce heating and prevent photodamage to trapped samples. Given the high intensities at the trap center, even moderate laser powers (e.g. 100 mW) can produce intensities exceeding $10^{11}\mathtt{W/m}^2$, which can be compared to the ca $10^{3}\mathtt{W/m}^2$ which the sun generates on a bright day, it is not surprising that it can harm biological samples or sensitive molecules [18].

Assuming the purpose of the tweezers is not only to position trapped objects, but also to study their dynamics, one needs to be able to track their motion at high sampling rates. A fast camera can suffice and is a simple solution since it can be used to track objects in the trap, and thus directly observe their movement. However, sufficiently fast cameras can be expensive and require relatively advanced analysis of the data obtained in the form of object tracking as well as powerful illumination. Therefore, most often one also adds a detector for the laser in the back focal plane, see fig. 1.2. This detector is usually a quadrant photodiode (QPD) or a position sensitive detector (PSD). These two types of detectors measure both the intensity, and the position, of light focused on them. Though their main functionality is the same, their construction differs a bit. A QPD is constructed from four photodiodes close together, and the position of the laser is calculated from the relative intensity of the different photodiodes. A PSD by contrast uses a PIN diode and measures four different photocurrents (two if it is a 1D PSD). Even though the performance of QPDs and PSDs is similar, a PSD is sometimes preferred since it is less sensitive to the size of the beam [19].

In terms of imaging, optical tweezers can integrate most common mi-

croscopy modalities. Brightfield imaging is commonly employed as it is both versatile and easy to integrate, as shown in fig. 1.2. High numerical aperture objectives in tweezers systems enable the incorporation of advanced imaging methods, including single-molecule fluorescence microscopy [16].

There are also several practical considerations that are rarely mentioned in scientific papers, but are essential to making a tweezers experiment work. Not least sample design, preparation, and manipulation. Problems with sample preparation can easily become costly in terms of research time. Either particles get stuck on surfaces or the sample starts leaking, causing unwanted flows. Typically, one also needs to be able to move the sample to position the optical trap on the object to be trapped. Manual handling is generally too imprecise; instead, samples are most often manipulated using manual or motorized micrometer translation stages, which provide superior accuracy and stability.

1.3.1 Expanding the capabilities of optical tweezers

Optical tweezers setups frequently incorporate additional functionalities to enhance performance or widen the range of applications. Common upgrades include precise steering of the trapping laser beam, high-accuracy control of the sample stage, and implementation of multiple optical traps that can simultaneously manipulate several particles [6, 20].

One of the most common extensions of standard optical tweezers is to include beam steering, the ability to precisely and dynamically control the laser position. This enables the accurate positioning of particles as well as the measurement of force as a function of distance, essential for instance in single-molecule applications, see section 2.1. Beam steering can be implemented in multiple different ways. The simplest is to use optical components such as movable mirrors, or the wiggler system employed in the MiniTweezers system as described in section 3.2, that translate the laser in the sample. These methods offer good control. However, since mechanical components are moved, their feedback speed is somewhat limited.

A common use of optical tweezers is to investigate how particles interact, or, as in the case of single-molecule experiments, tether two particles together with a molecule [8]. Such applications require multiple particles, and one attractive way to achieve this is to use multiple optical traps. There are many methods for generating multiple traps in an optical tweezers [21], the conceptually simplest of which is to add another laser. However, since lasers and optics to collimate them and combine beams are expensive and complicated, it is common to instead split a single laser into multiple differ-

ent traps. Again, there are many different ways of doing this, one can for instance use a simple beam-splitter and split by polarization and then move the beams individually. However, independent control of all the different beams is sometimes desired. A good option can then be an acousto-optic deflector (AOD) which acts by quickly moving the trapping beam along a single axis. The update frequency is generally a few MHz, much faster than the trapping dynamics, and thus by moving the optical trap very rapidly a single laser is used to create several movable traps [22]. This has the additional advantage that there is no risk that the different traps interfere since they are temporally independent. Furthermore, because they follow the same optical path, one can also achieve great stability with them [23].

The perhaps most versatile method for creating multiple optical traps is achieved with holographic optical tweezers [20, 24]. These use a Spatial Light Modulator (SLM) to create multiple traps. An SLM works similarly to a computer screen, but instead of the pixels of the screen displaying different colors, they either change the phase or the intensity of the light hitting it. This is used in optical tweezers to create steerable optical traps by sculpting the wavefront of the laser so that it creates multiple focal points in the sample. This gives an unprecedented flexibility by being able to create several traps which can be moved freely and with high precision in 3D. However, it comes with the drawback of significantly reduced laser power. Furthermore, the algorithms used for creating the holograms are computationally quite demanding, especially when creating multiple traps. The SLM units are also often expensive and update frequencies rarely exceed 100 Hz and they require additional optical components (primarily lenses and mirrors) which increase the complexity of assembly and alignment.

One can also extend optical tweezers by adding functionality beyond that of trapping. Integrating advanced imaging or sensing techniques further expands the versatility of optical tweezers systems. Notably, fluorescence microscopy, Raman spectroscopy, and interferometric detection methods have been successfully combined with optical traps to simultaneously manipulate and probe single-molecules, cells, or particles [16, 25]. Another addition, which is often of interest, is temperature control. Temperature affects biological, physical and chemical processes. For instance, measurements of critical Casimir forces is a prime example of an application that requires accurate temperature control [26]. In our lab, we integrated temperature control by insulating the environment around the sample with plastic foam and using a thermoelectric element attached to the objective for accurate temperature control.

1.4 Calibration of optical tweezers

The goal of many optical tweezers experiments is to relate quantities such as forces, energies, and positions to various physical phenomena, e.g. for quantifying critical Casimir forces or the energy required to unfold a protein. However, the signals from an optical tweezers usually come from either a quadrant photodiode or from a position sensitive detector, which monitors how the trapped particle affects the trapping laser. These detectors will output an electrical signal, not a force or position. The signal therefore needs to be converted into either a position of the trapped particle or the force acting on it (often both are needed). Calibration refers to the process of finding a mapping from sensor readings to particle position, and by extension also the force from the trap acting on the trapped particle. In cases when a camera is used to study particle motion, the output is instead a position in pixels and the translation to position is straightforward, one simply needs to measure the pixel size which can be done with a micrometer ruler, but there is still often a need to convert displacement from the equilibrium position in the trap to a force. This still requires calibration (determining the stiffness in eq. (1.1)).

There are several calibration methods, such as the Stokes drag method, power spectral density, potential analysis, and FORMA [6,27]. The method that is most suitable depends on the trapping configuration and the sensor capabilities. In this section the Stokes drag method, which is used to calibrate the system used in papers II and III, is described and the generalized version of FORMA, introduced in Paper IV, is outlined.

1.4.1 Stokes drag

One of the most straightforward methods for calibrating an optical tweezers is the Stokes drag method [6]. It is also the method used to calibrate the SmartTrap system used in papers II and III.

As the name suggests, this method utilizes Stokes' law that relates the viscous force, $\vec{F_v}$, acting on an object with hydrodynamic radius, R, to the fluid velocity $\vec{v}$ and viscosity η [28].

$$\vec{F_v} = -6\pi\eta R\vec{v} \tag{1.2}$$

By trapping a particle and moving the trap at a known velocity through the sample, one can relate the particle deflection, or QPD/PSD reading, to the viscous force. By setting the viscous force equal to the force from the

optical tweezers we get.

$$\vec{F_o} = \vec{F_v} \tag{1.3}$$

Importantly, there is also Brownian motion, which is why there can be short-term deviations, but eq. (1.3) holds in average.

The Stokes drag method can be used for calibration when both the particle sizes and the medium viscosity are well known during calibration. In practice, it is most often used when the instrument is used for direct force measurements through measurement of the momentum change of light. This is because when measuring the momentum change the force is always linearly proportional to the laser deflection (multiplied with the power which is also measured) and therefore only a single force and a single sensor reading are needed for calibration. In most single beam optical traps it is not possible to collect enough of the trapping light scattered by the trapped object to get an accurate estimate of the momentum change of the laser. Therefore, other calibration methods, such as potential analysis, are employed.

When performing a calibration using the Stokes drag method, multiple different particles are often used, and they are moved along all the movement axis of the instrument to account for variations in particle size and in sensitivity of the sensor/electronics. Furthermore, since experiments are performed in a microfluidics chamber with finite depth, the walls of the chamber will affect the force slightly. One can compensate for this by using the first-order correction from [29] which accounts for the thickness of the sample cell by multiplying the force with a factor $\frac{9r}{16d}$ where d is the distance to the wall and r the particle radii. If there is more than one wall nearby, the correction is applied multiple times.

Usage in the MiniTweezers system

The Stokes drag method is used to calibrate the MiniTweezers system, as it uses direct force measurement and has a motorized sample stage which allows for easy generation of drag forces. The system needs six different calibration factors. One for each axis of each laser. The trapped particle is moved back and forth at between different positions and along the three main axes (x,y and z) thereby creating the Stokes drag. Moving along the x-axis, we get the following relation

$$F_{vx} = \alpha_x PSD_{ax} + \beta_x PSD_{bx} \tag{1.4}$$

Where PSD_{ax} is the reading of PSD force detector a in the x-direction and α_x the corresponding sensitivity coefficient. PSD_{ax} and β_x are the corresponding values for laser b. The force along y is calculated analogously.

However, the force along the axial direction is calculated slightly differently because it is directed along the propagation axis of the lasers. For this axis, we get the force as

$$F_{vz} = \alpha_z \frac{I_a}{S_a} + \beta_z \frac{I_b}{S_b} + O_z \tag{1.5}$$

Where I_a is the iris reading and S_a is the sum (e.g. power) reading of laser a. Again, α_z and β_z are calibration factors. The constant O_z compensates for the zero offset of the readings.

There will be slight differences in the different coefficients due to variations in the sensitivity of the different PSDs, the electronics (e.g. amplifiers, connectors, and resistors), and optical path. Nonetheless, coefficients tend to be the same within a couple of percent, with the exception of the coefficients for the z-axis in eq. (1.5). The system is calibrated by setting the two lasers to equal power (as measured after passing through the sample) where the two traps have equal efficiency. This means that $\alpha_x PSD_{ax} = \beta_x PSD_{bx}$. Lastly, the calibration is verified by performing a DNA pulling experiment where an overstretching plateau at ca 65 pN confirms that the calibration is accurate.

1.4.2 FORMA and the problems of long integration times

Force Reconstruction via Maximum-Likelihood-Estimator Analysis, or FORMA for short, is a relatively new calibration method which makes use of a maximum likelihood estimator for finding optical trap stiffness and diffusion constant [27]. This method is appealing in that it does not require long trajectories and could achieve high accuracy if the sampling rate is high. Here, a high sampling rate means a sample rate about an order of magnitude higher than the corner frequency of the optical trap. With FORMA the optical trap stiffness κ is estimated as

$$\kappa = -\gamma \frac{\sum_{n=1}^{N_s-1} x_n \frac{x_{n+1}-x_n}{\Delta t}}{\sum_{n=1}^{N_s-1} (x_n)^2} \tag{1.6}$$

Where N_s is the number of samples, x_n are the sampled positions and Δt the time between samples. $\gamma = 6\pi\eta R$ is the particle drag coefficient with η the dynamic viscosity and R the particle radius. Furthermore FORMA also

gives the diffusion coefficient D as

$$D = \frac{\Delta t}{2(N_s - 1)} \sum_{n=1}^{N_s - 1} \left(\frac{x_{n+1} - x_n}{\Delta t} + \frac{\kappa}{\gamma} x_n \right)^2 \tag{1.7}$$

However, it is not always possible to reach the high sampling rates required, especially when using a camera and limited illumination, which for instance can be the case when trapping fluorescent samples. Then you need to use long exposure times, also known as integration times δ, to achieve sufficiently high signal-to-noise ratio to be able to track the trapped particle's motion. This limits the maximum sample rate to $1/\delta$. However, a low sample rate is not the only issue introduced when using a long integration time.

Using a long integration time with the acquisition device (e.g. camera or QPD) causes a smoothing of the signal, similar to low-pass filtering. This effect is illustrated graphically in fig. 1.3 a. It makes particles appear closer to the trap than is actually the case, as can be seen also in the simulated trajectories in fig. 1.3 b. This effect is not considered in standard calibration methods, nor in the original FORMA. It gives the perception of a stiffer trap (larger κ) and lower diffusion coefficient D.

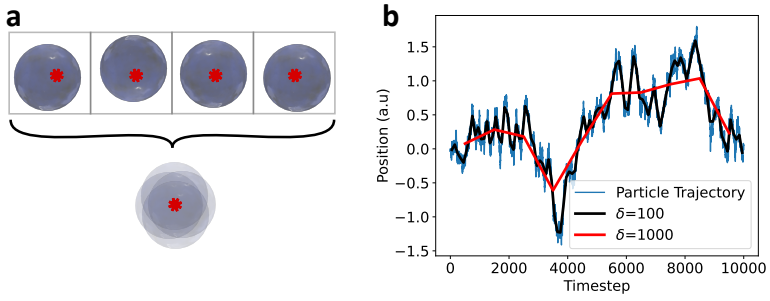

Figure 1.3: **Illustrations of the problems which occur when using long integration time for calibration.** **a** When the particle moves around in the trap the sampled position will be the average of the position during the integration time resulting in a *blurred* image in which the particle appears closer to the central position. **b** The blue line shows a simulated trajectory of a particle. The black and red shows the same trajectory but sampled with longer integration times , 100 timesteps for the black and 1000 for the red.

In Paper IV, FORMA, as well as the Mean Squared Displacement, Equipartition, Power Spectral Density and Autocorrelation Function methods, were generalized to account also for limited sampling rates and the motion blur induced by long integration times [30]. The generalized methods compensate for the integration time by accounting for the fact that the samples are taken from a different distribution than what is assumed in standard calibration methods. This is done by making use of the fact that the trajectory positions sampled $\tilde{x}_n$ can be viewed as an integral of the true trajectory during an interval of δ.

$$\tilde{x}_n = \frac{1}{\delta}\int_{t_n-\delta/2}^{t_n+\delta/2} x(t)dt \tag{1.8}$$

The full derivation of the various generalized calibration methods is rather technical, especially that of FORMA, and can be found in Paper IV. Here we present how the formulas in eq. (1.6) and eq. (1.7) are modified. First we define the relaxation time of the optical trap $\tau_{ot} = \gamma/\kappa$ and the parameter $\alpha = \delta/2\tau_{ot}$ the latter can be seen as a measure of the influence of the integration time on the sampling. The generalized equations can then be written as

$$\mathcal{F}(\alpha) = \frac{e^{-2\alpha} + 2\alpha - 1}{2\alpha^2} \tag{1.9}$$

$$\mathcal{G}(\alpha)e^{-\Delta t/\tau_{ot}} = \frac{\mathcal{T}_2}{\mathcal{T}_3} \tag{1.10}$$

$$\frac{k_bT}{\kappa}\mathcal{F}(\alpha) = \frac{\mathcal{T}_1 - \frac{\mathcal{T}_2^2}{\mathcal{T}_3}}{1 - (\frac{\mathcal{T}_2}{\mathcal{T}_3})^2} \tag{1.11}$$

$$\mathcal{G}(\alpha) = \frac{\left[\frac{\sinh(\alpha)}{\alpha}\right]^2}{\mathcal{F}(\alpha)} \tag{1.12}$$

Where we have introduced the estimators $\mathcal{T}_1$, $\mathcal{T}_2$ and $\mathcal{T}_3$ defined as

$$\mathcal{T}_1 = \frac{1}{N_s - 1}\sum_{n=1}^{N_s-1}[\tilde{x}_{n+1}]^2 \tag{1.13}$$

$$\mathcal{T}_2 = \frac{1}{N_s - 1}\sum_{n=1}^{N_s-1}[\tilde{x}_{n+1}\tilde{x}_n] \tag{1.14}$$

$$\mathcal{T}_3 = \frac{1}{N_s - 1}\sum_{n=1}^{N_s-1}[\tilde{x}_n]^2 \tag{1.15}$$

The equations are solved numerically, yielding accurate estimates for κ and D, also in conditions which are far from ideal. The generalized version of FORMA performs very well for estimating both the trap stiffness and the diffusion constant. When using either a QPD or a PSD to sample the particle trajectory, the integration time is generally short enough (and perhaps not even known) so one does not need to use the generalized methods, but when the integration time is long it is crucial to do so as was shown in Paper IV.

1.5 Digital video microscopy

When operating any microscope there is always a large reliance on what is seen to operate the instrument. This is especially true for optical tweezers, where the sample must be positioned not only for imaging but also for trapping and studying objects. Steering the instrument is often challenging, and researchers often want to extract quantitative data (e.g. the number of cells, fluorophores, and trajectories of particles) from microscopy images or videos analyzed systematically. This has given rise to the field of digital video microscopy (DVM) in which images are analyzed digitally.

Interpreting images from a microscope is rarely trivial. Images are often complex and the requirements for precision are high, which has led to a range of different specialized approaches to tackle different situations. In the context of optical tweezers, DVM is typically used to track the motion of trapped particles. In this way, one can calculate the position of the particle with nanometer precision directly from a video recording. Calibration to get the particle position is in this case very simple, requiring only a conversion factor relating pixels to microns. This conversion factor can be obtained by installing a micrometer ruler in the system and measuring the distance. Challenges lie instead in attaining sufficiently high frame-rates (order of kilohertz).

There are multiple different approaches to particle localization such as thresholding, radial symmetry and various deep learning approaches [31]. Deep learning is more versatile than other methods and with the rapid development of new methods we are likely to see increasingly widespread adoption in the future as discussed in Paper I. Since deep learning is used in three of the four papers presented in this thesis, it is also the class of methods which is in focus here.

1.6 Particle tracking with deep learning

In recent years, deep learning has emerged as the primary method for detecting particles, offering superior sensitivity and flexibility compared to other methods [32, 33]. Because of this, it is becoming increasingly common for optical tweezers applications [34]. Within deep learning, there are multiple different approaches to particle tracking utilizing different architectures. Most are based on convolutional neural networks (CNNs). Commonly used architectures include standard CNNs, U-Nets, and YOLO, all of which are applied in Paper II. These different networks have been designed to tackle different challenges, the YOLO algorithm is, for instance, designed to be fast. Here we give a brief introduction to these methods, focusing on their strengths and weaknesses and how this affects which applications they are suitable for.

1.6.1 Convolutional neural networks

Convolutional neural networks (CNNs) have become a cornerstone of modern computer vision. Their ability to efficiently capture spatial hierarchies and long-range correlations between pixels makes them especially well suited for analyzing image data [35]. This capability arises from the use of convolutional layers, which systematically apply learnable filters (or kernels) across the input image. The convolution operation is illustrated in fig. 1.4a.

During convolution, the image is divided into small overlapping patches, such as 3×3 pixels as shown in fig. 1.4 a. Each patch is element-wise multiplied by a kernel, and the resulting values are then summed to produce a single number. Typically, each convolutional layer contains multiple kernels, which are learned during training and enable the network to detect different features. The stride determines the distance between the centers of adjacent patches and can be adjusted to control the spatial resolution in subsequent layers.

A typical CNN architecture, as depicted in fig. 1.4b, contains several types of layers: convolutional layers, pooling layers, and fully connected (dense) layers. Pooling layers, such as max pooling, help reduce the spatial dimensions of the feature maps and emphasize important features. Like convolution, pooling operates on patches, but instead of applying a learned kernel, it extracts a simple statistic, most commonly the maximum value in each patch.

Dense layers are typically used for the output of the network. After feature extraction by the convolutional and pooling layers, the resulting

feature maps are flattened into a one-dimensional vector. Each neuron in a dense layer is connected to every output from the previous layer. The output of a neuron in a dense layer is given by

$$y = f\left(\sum_i w_i x_i + b\right), \tag{1.16}$$

where x_i are the inputs, w_i are the learnable weights, b is a bias term, and f is a nonlinear activation function (such as ReLU or sigmoid) [35]. These layers combine and interpret the high-level features extracted by the convolutional layers, enabling the network to perform tasks such as classification or regression.

Convolutional layers serve as powerful feature extractors, detecting local patterns such as edges, corners, and textures by leveraging the spatial locality in images. Through multiple layers, CNNs build hierarchical feature representations: early layers typically identify simple, low-level patterns, while deeper layers combine these to recognize more complex, abstract structures [36]. In the example in fig. 1.4a, the kernel emphasizes regions with horizontal lines, illustrating how kernels specialize to detect specific patterns during learning. This layered approach forms the backbone of advanced neural network architectures and is fundamental to contemporary deep learning applications.

CNNs have achieved remarkable success in a variety of applications. Notably, their breakthrough performance in the ImageNet Large Scale Visual Recognition Challenge (ILSVRC) demonstrated their capacity to outperform traditional computer vision methods by a large margin [37]. Since then, CNNs have become the standard approach for tasks such as image classification, object detection and semantic segmentation.

In Paper II a CNN was used for determining the axial position of particles. The choice fell naturally on this architecture since it is both simple and effective. However, since in this case the network was trained from scratch, large amounts of training data were needed. We made use of simulated data for this, in particular we used the DeepTrack2 package [38]. However, we did encounter trouble with the mismatch between experiments and the simulated data, which meant that a significant amount of fine-tuning was needed for good performance. To simplify for the network, the predictions are made on crops of the image centered around the particle detections, this reduces the influence of random noise outside the particle itself.

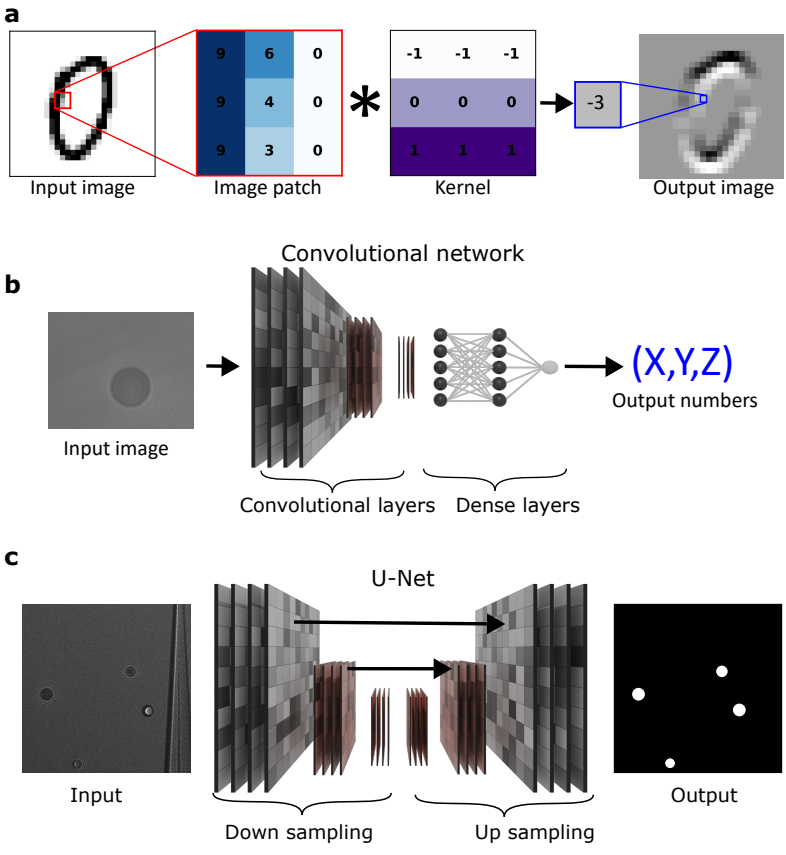

Figure 1.4: **Artificial neural networks used in image analysis. a** Illustration of how a convolution works. The input image is split into patches, each of which is multiplied elementwise by the kernel and then added together to produce a single number. **b** A convolutional neural network consists of first a set of convolutional layers (and often with pooling in between) followed by a small dense network. The network takes images as inputs and outputs one or several numbers. When used in a convolutional neural network the convolutions are often paired with pooling as well. **c** An illustration of the U-net architecture. The U-Net takes as input images and outputs images, transforming the input image by a series of convolutions and poolings.

1.6.2 U-Nets for multi-particle tracking

Image segmentation, the task of assigning pixels in an image to a specific class, is today dominated by deep learning. The U-Net architecture and its variants are among the most widely used in biomimaging [39]. The U-Net architecture gets its name from the shape, there are several convolutional layers of decreasing size stacked which compress the data, followed by layers of increasing size that up-sample it as illustrated in fig. 1.4 c [40]. There are also residual connections going between the downsampling and upsamling paths whose purpose is to help the network maintain details. The idea is that the residual and shallow layers should help the network detect details while the deeper layers should look at larger scale structures. Since U-Nets were introduced a decade ago, they have had great success in various segmentation tasks within bio-imaging, with applications ranging from CT-scans to electron microscopy [40, 41].

The U-Net works by taking one image as input and converting it into a heat map that classifies features of the image, such as the particle positions shown in the output image of fig. 1.4 c. Taking particle tracking as an example, the U-Net should output a heatmap that has values proportional to the likelihood that there is a particle in each pixel. Extending this to several different types of particles is straightforward; the network is simply modified to output several different images (or channels), each corresponding to a specific type of particle. To get particle positions from the U-Net predictions, one needs to analyze the heatmaps to convert them into actual particle localizations. This is done by thresholding and finding the centers of mass for the different connected segments.

In our optical tweezers experiments, and the adsorption experiments in particular, the U-Net proved very useful for accurate particle tracking. Since we lack knowledge of the true particle positions in our experimental data it is difficult to use it for training a neural network, especially if high accuracy is needed. Instead, we employed simulated data from the DeepTrack2 package [38] to simulate the particles. In this way the network was able to account also for the particles being partially immersed in the oil droplets by having sufficiently varied training data. In particular training data in which particles of different sizes overlapped.

1.6.3 YOLO object detection

Object detection is the task of locating objects in images or videos. If the purpose is to analyze video, especially in real-time, then there is also a need

for the algorithms to be fast. The large number of industrial applications, ranging from facial recognition, reading number plates, etc, have given rise to a large number of different algorithms and one of the most used ones are YOLO (You Only Look Once) [42, 43]. This architecture predicts so-called bounding boxes, which both classifies and encompasses the different objects in an image.

The YOLO algorithm, and subsequent improvements to it, are publicly available through Ultralytics [44]. This easy availability is one of the main reasons for using it. Furthermore, it can also be trained to high accuracy with relatively little training data thanks to the use of transfer learning. In Paper II the network was trained on roughly 1000 images, but still achieved accuracy superior to that of the U-Net. Lastly, of course, the speed of the network has been key to its widespread adoption. This comes from YOLO using only a single, relatively simple forward pass to perform the predictions. The U-Net for comparison requires a post-processing step for object detection and by retaining the original size of the image at the output the predictions from network itself are also computationally demanding to calculate. The biggest drawback with YOLO for our applications in Paper II is perhaps that it struggles with very high object densities (many objects in a small area), a situation rarely encountered during our experiments. Furthermore, as noted in Paper II, the precision has also been lower than that of other methods, such as U-Nets, but this is likely due to the inclusion of manually annotated data, a more dedicated push towards accuracy could probably alleviate these issues. Using a newer and larger version of YOLO might help with these problems but would be more computationally demanding and thus slower, which is a trade-off that is likely not worth it for the real-time applications.

1.7 My contributions to optical tweezers

During my PhD optical tweezers have continually played a central role, forming a common thread throughout this thesis. My work has been primarily experimental, focusing on applying tweezers to novel problems in biophysics and colloidal chemistry. The background to the problems tackled is presented in chapter 2. However, most of my time in the lab was not spent directly performing measurements, but rather on developing new techniques, improving existing ones, and analyzing data. I spent countless hours in the lab assembling optical tweezers, refining alignment, and testing new experimental protocols.

The single largest part of the work was devoted to construction of a MiniTweezers and the refinement of this into the SmartTrap system. This system and how it works are described in Chapter 3. The chapter is also intended to act like a starting point for those seeking to build on the new hardware and software of the SmartTrap, or develop their own systems.

Another key component of experimental work is data analysis. It is during the analysis that one discovers how high quality the data are, which in the context of optical tweezers, means consistently performed experiments with low noise and bias. High quality data are central also when training machine learning algorithms, for which large amounts of data are generally needed. It is worth putting in the time to refine procedures to get good data, as was needed for both Paper II and III. Having reliable methods for analyzing data is important, not only for understanding the results of experiments, but also for automation where it is used to make decisions in real time. Chapter 4 complements chapter 3 focusing on the algorithms used for automation. The chapter is meant to be an introduction to automation in biophysics and the methods used in Paper II, offering a practical and accessible take on the subject.

It is both my hope and belief that the system and methods I have helped develop will continue to improve and be used. If your methods work, and are well designed, people will continue using them for decades, as was the case with the original MiniTweezers.

Chapter 2

Applications of optical tweezers

Optical tweezers have numerous applications in a variety of scientific fields such as biophysics, colloidal chemistry, and quantum physics [6, 21, 45]. The popularity of optical tweezers comes from their unique ability to provide non-contact, highly precise manipulation of objects at the micro- and nanoscale, a task for which there are few other methods [7, 15, 16, 45]. Additionally, optical tweezers enable simultaneous measurement of forces at the piconewton scale, making them invaluable tools for studying the mechanics of small systems. Some of the most prominent and impactful applications are in biophysics, contributions to which earned Arthur Ashkin the Nobel Prize in Physics in 2018 [10]. In this chapter, we introduce the main applications of optical tweezers as explored in the papers presented in this thesis, with particular emphasis on the associated experimental considerations.

2.1 Single-molecule experiments

One of the most exciting possibilities offered by optical tweezers is the ability to study the behavior of single molecules. The keyword here is **single**. There are multiple bulk methods for studying biomolecules, such as calorimetry and surface plasmon resonance, but these risk missing the dynamics of process, which can be key to understanding [46]. In particular, bulk methods struggle when dealing with heterogeneous processes since they often yield just an average value from many processes. Understanding biological pro-

cesses at the single-molecule level is key to establishing a complete picture of biomolecular processes such as the workings of molecular motors and for understanding microthermodynamics [47].

Still, optical tweezers are not the only single-molecule technique, atomic force microscopy and magnetic tweezers are also commonly used [45], but optical tweezers are the most widely used because of the precision and high temporal resolution offered in measurements and positioning. In particular, the possibility to study how molecules behave when a force is applied to them, what is known as single-molecule force spectroscopy, is something optical tweezers excel at. These experiments are most often performed by attaching the ends of the molecule of interest between two micrometer-sized particles. One (or both) of the particles is held in an optical tweezers. The trapped particle is used to both apply and measure forces on the molecule. In the standard experiments the trapped particle is moved between two set positions, generating a graph of the force as function of distance (or molecular extension), but as we shall see also other protocols are used.

Exploring DNA dynamics with single-molecule force spectroscopy

Single-molecule force spectroscopy is when the force is studied as a function of molecular extension. In the case of optical tweezers, the field dates back to the 1990s and the group of Carlos Bustamante. They were the first to use optical tweezers to study in detail how DNA behaves when it is stretched by forces applied to the ends of the molecule [48]. Thus, they established that the extension of double-stranded DNA can be well described by the extensible worm-like chain model. Nowadays, the field of single-molecules has shifted attention towards molecules with more complex behaviour, such as DNA-hairpins, RNA and proteins as well as more complex experiments to investigate processes such as DNA replication, transcription and protein folding [8, 49]. However, the results of the DNA pulling experiments remain key to understanding other experiments. This is largely because DNA handles are used to connect molecules, such as proteins or DNA hairpins, to microparticles. Then, when the target molecules are pulled, one needs to take into account also the stretching of the DNA handles, which requires a proper understanding of the DNA dynamics [8].

The DNA pulling experiments helped establish that force-extension dynamics of DNA can be modeled using the worm-like chain model (WLC model). The WLC model assumes that the polymer can be characterized by two parameters, the total length of the polymer (the contour length) and the persistence length [50]. The persistence length can be viewed as a mea-

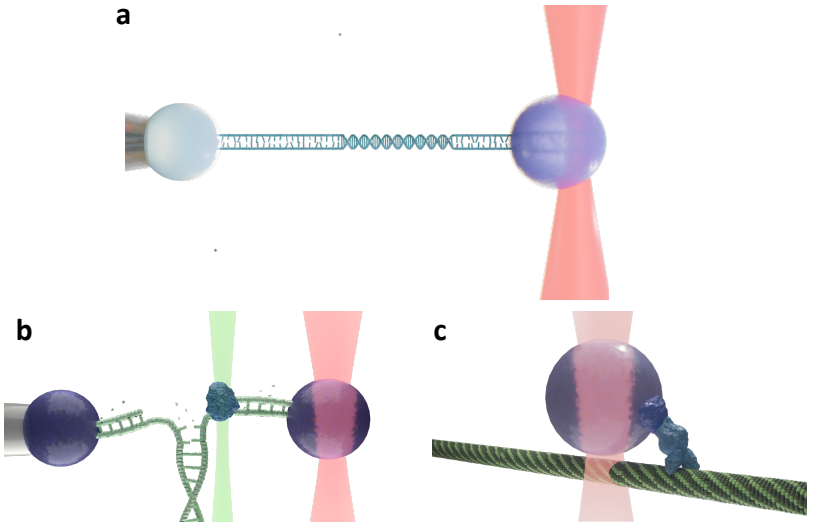

Figure 2.1: **Illustrations of various single-molecule experiments**. **a** In DNA pulling experiment single molecules are tethered between two microparticles, one of which is held in an optical trap. The optical trap is moved, applying a force on the trapped particle. **b** By incorporating a secondary excitation laser one can measure when and where proteins bind to molecules. **c** Measurement of the stepping of a molecular motor on microtubule. The molecular motor is attached to a particle held in an optical trap. When the motor moves along the microtubule, the stepping of the motor is observed on the movement of the particle.

sure of the bending stiffness of the polymer. Stiffer molecules have greater persistence lengths; e.g. double-stranded DNA is stiffer than singe-stranded DNA and therefore has a longer persistence length. Furthermore, the model describes the polymer as moving and bending freely, only influenced by Brownian motion and the inherent stiffness. However, entropy will make the polymer coil up to just a fraction of the contour length, counteracting stretching of the molecule.

The WLC model can be used to describe the force, F, required to stretch a molecule a distance x or equivalently the relative extension $\mathrm{E} = \frac{x}{L_0}$ where L_0 is the contour length of the molecule as illustrated in fig. 2.2. The derivation of the force as function of distance is somewhat technical, see [51].

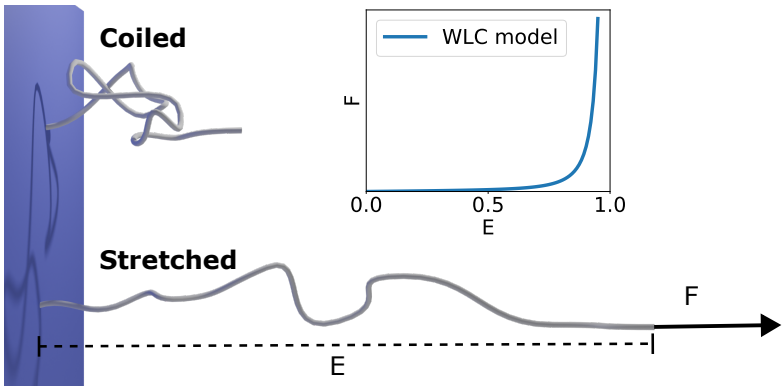

Figure 2.2: **Illustration of the worm-like chain model.** The model can describe the force, F, required to stretch a polymer from a coiled state (top) to a stretched state (bottom). The inset shows the force as a function of molecular extension, E, relative to the contour length of the polymer. The force diverges as the extension approaches the molecule's contour length.

It yields the following expression for the force

$$F(x) = \frac{k_\mathrm{b}T}{L_\mathrm{p}} \frac{1}{4(1 - x/L_0)^2} - \frac{1}{4} + \frac{x}{L_0} \tag{2.1}$$

Where $k_\mathrm{b}T$ is the Boltzmann constant, T the temperature, L_p is the persistence of the molecule. However, for high forces, eq. (2.1) fails to describe the extension accurately. This is because the molecule itself will stretch, and the equation needs to be modified to account for this enthalpic contribution. It can be shown that this can be accounted for by changing $x/L_0 \rightarrow \frac{x}{L_0} - \frac{F}{K_0}$ where K_0 is the stretch modulus of the molecule [52]. One thus arrives at the following expression for the *extensible* worm-like chain model.

$$F(x) = \frac{k_\mathrm{b}T}{L_\mathrm{p}} \frac{1}{4(1 - x/L_0 + F/K_0)^2} - \frac{1}{4} + \frac{x}{L_0} - \frac{F}{K_0} \tag{2.2}$$

The stretch modulus of double-stranded DNA has a value of ca 1200 while the persistence length is around 43 nm [9]. As we see in Paper III the model can also describe the extension of synthetic polymers, even though these are much less stiff (a persistence length of less than 1 nm was found in Paper III).

Protein folding and unfolding

Another fundamental category of biomolecules that is often studied with optical tweezers are proteins. Using experimental configurations similar to those used in DNA pulling one can study protein folding and unfolding [53]. Unlike bulk methods, the high resolution of optical tweezers makes it possible to study folding intermediates (partially folded proteins), and in particular, if they are on or off the folding pathway [8]. Most often a force ramp protocol is used for protein pulling experiments e.g. the particle is moved between two fixed positions. However, also other protocols, such as constant force and constant position, are sometimes used, enabling researchers to study phenomena such as hopping between folded and unfolded states.

Looking ahead, the study of protein folding may very well be the optical tweezers application that sees the most growth in the future. This is because protein folding with optical tweezers is starting to find use in the development of new drugs, enabling researchers to dynamically study the effects of drugs on target proteins [54]. Furthermore, since the observation of misfolding and folding intermediates require data, it is likely that autonomous algorithms, such as those described in this thesis, could be used to discover rare, or short-lived, intermediates and to search for these in a systematic manner.

Molecular motors

The excellent control of particles enabled by optical tweezers also unlocks different types of experiments using other types of feedback and different biological assays. In particular, one can study the operation of molecular motors. One of the first motors studied was kinesin and this soon led to the observation of kinesin stepping [55, 56]. This was the first direct demonstration that molecular motors move using discrete steps, rather than continuously. With optical tweezers it is also possible to measure the stepping length of the motors, which in the case of kinesin are 8 nm long. By pushing the resolution limit with an ultra-stable dual trap optical tweezers, single-base-pair stepping was observed in RNA polymerase [57].

Another property that one can easily extract from optical tweezers measurements is the stall force, which is the force required to stop a molecular motor. In the case of RNA polymerase, which transcribes DNA into RNA, the stall force was found to be 14 pN [58]. These are just a few of the molecular motors that have been studied with optical tweezers, there are multiple other, such as ClpX unfoldase, bacteriophage ϕ29 DNA packaging motor and the muscle protein myosin to name a few [59–61].

Many of these experiments are rather challenging to perform, requiring the handling and assembly of multiple large proteins as well as very high-resolution optical tweezers [9]. They could therefore potentially benefit from being automated using protocols similar to those presented in Paper II since this can increase the accuracy of the control and repeatability of the experiments. However, in cases where not much data are needed, it may very well be faster to perform the experiments manually rather than adapting an autonomous protocol.

2.2 Single cells

Optical tweezers are particularly suited for manipulating objects at the micrometer scale, making them powerful tools for probing the mechanics and behavior of single cells. Their ability to apply and measure forces in the pico- to nano-newton range allows for precise and non-invasive manipulation, which has led to extensive use in biophysical studies of single cells and their mechanical properties [7, 62]. In recent years, the increasing automation and integration of systems with microfluidics and imaging modalities such as FRET has further enhanced their applicability in single-cell research [63].

2.2.1 Red blood cell deformability

Red blood cells (RBCs) have been extensively studied using optical tweezers because of their soft membranes, which make them easy to stretch, and their close link to biomedical applications. In particular, the link to certain diseases such as sickle cell disease makes understanding them important. Optical tweezers have been used extensively to quantify their deformability, membrane elasticity, and response to mechanical stress [7,64]. Several different trapping configurations have been used to stretch RBC. There are dual trap configurations with two microparticles as handles and also a single trap configuration using the momentum change of the laser as it passes through the cell for stretching, as well as a dual trap in which the two traps are used to pull the cell [65–67].

In the dual-particle configuration, two microparticles are attached to opposite ends of a single RBC, somewhat similar to the configuration used for single-molecules. These particles are then optically manipulated to stretch the cell. The trapped particles serve as handles for precise control and tracking, allowing researchers to derive mechanical parameters such as membrane shear modulus and viscoelasticity. This configuration has also been used in

the MiniTweezers [66]. The method provides a simple means for measuring the applied forces (same as in other optical tweezers configurations) and the lasers do not pass through the cell limiting photodamage. The main disadvantage is that it is not non-contact and is relatively low throughput compared to some of the alternative methods.

In contrast, direct optical deformation of cells, known as the optical stretcher, focuses two laser beams directly on the cell to induce shape changes via optical stress. This method is non-contact, which reduces experimental complexity, and avoids mechanical artifacts from particle-cell adhesion [65]. However, quantifying the forces involved in such configurations is challenging. It often requires detailed simulations of light propagation through cells to estimate the optical forces involved. Recently, another non-contact method was used in which two different traps were employed to grab parts of the red blood cells to systematically stretch the cells and then relax them [67]. The cells were showing long term hysteresis, becoming gradually stiffer the more times they were stretched.

2.2.2 Other cell types, subcellular units and future applications

The membrane mechanics of other cell types, such as yeast cells and breast epithelial cells, have been studied with optical tweezers [68]. However, there are many applications of optical tweezers to single-cell studies which investigate phenomena other than membrane mechanics.

Optical tweezers ability to manipulate cells in a non-contact manner is highly appealing, offering a straightforward method for positioning and sorting cells [7]. By holding single cells in the optical trap one can measure the properties of them as the media is changed.

Considering the recent rise machine learning, discussed in Paper I, it seems all but certain that it will be applied also to optical tweezers and single cells beyond the example we show in Paper II. Machine learning has potential not only in the analysis, where it has already seen widespread adoption [69], but it could also power automation. Using machine learning (and in particular for image analysis) could help guide the tweezers and monitor, or measure, properties over long periods of time or to look for rare events. For example, selecting and specific bacteria species in a natural sample containing a large variety of different species at different concentrations (somewhat similar to the particle characterization introduced in Paper II). Then moving these bacteria to a separate area of the chamber to grow them selectively.

2.3 Optical tweezers in colloidal sciences

In the most general terms, colloids are microscopically insoluble particles dispersed in a medium, such as polystyrene particles in water. Colloidal particles typically refer to particles that range in size from a few nanometers to micrometers, which overlap well with the operational range of optical tweezers. This has led to optical tweezers quickly finding multiple applications to study phenomena such as diffusion, depletion interactions and polymer dynamics [70]. Some common colloidal measurements are illustrated in fig. 2.3, variations of which were performed in Papers II and III.

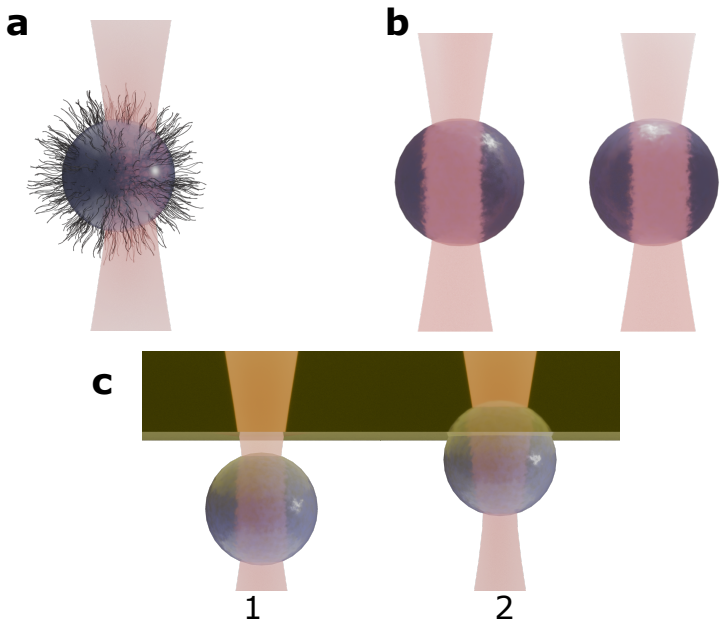

Figure 2.3: **Examples of colloidal measurements performed with optical tweezers. a** By trapping a particle and moving it at constant speed the size can be measured and the optical trap stiffness can be obtained by studying the particle's diffusion. **b** Interactions between particles can be studied by pushing particles together while simultaneously measuring the force between them. **c** By bringing a particle to a liquid-liquid interface (panel 1), such as oil-water, with optical tweezers the dynamics of adsorption (panel 2) can be studied with high resolution.

2.3.1 Particle-particle interactions

Colloidal particles are subject to a variety of interparticle forces that govern their stability and dynamics. In the absence of repulsive interactions, random Brownian collisions will inevitably lead to aggregation, primarily driven by attractive van der Waals forces [71]. To prevent this, colloids are typically "charge-stabilized", meaning that the particles are engineered to carry surface charges of the same sign, giving rise to electrostatic repulsion that keeps them apart. An alternative approach involves coating particles with polymer shells, which introduce steric hindrance, and an additional repulsive component that also suppresses aggregation [72].

Optical tweezers have become indispensable tools for investigating particle-particle interactions in colloidal systems. By trapping and manipulating single particles with high precision, tweezers allow direct measurement of the forces between them. A common experimental approach is to bring two particles together using one or two optical traps, as illustrated in fig. 2.3 **b**.

A particularly noteworthy application of optical tweezers is the measurement of critical Casimir forces. While the classical Casimir effect arises from quantum fluctuations between conducting plates [73], the critical Casimir force emerges in fluids near critical demixing points [74]. Hertlein *et al.* [75] directly measured the critical Casimir force between a colloidal particle and a planar wall in a binary liquid mixture using optical tweezers. Subsequent experiments extended these measurements to interactions between two particles, revealing the non-additive nature of the critical Casimir force [76]. These studies illustrate the versatility of optical tweezers for exploring fundamental interactions in soft matter, capable of measuring from simple charge-stabilized colloids to complex systems exhibiting many-body effects.

2.3.2 Adsorption of colloidal particles to liquid interfaces

The adsorption of colloidal particles to a liquid interface has received significant interest as it has applications ranging from drug delivery to mineral recovery [77]. Particles attached to a liquid-liquid interface can help stabilize the emulsion by forming Pickering emulsions. Even though optical tweezers are well suited for this since they can manipulate particles in a non-contact manner, they are still not widely used in this field.

There are some influential studies using optical tweezers which have focused on the dynamics of particles adsorbing into interfaces. This has been pioneered by the group of Manoharan [78, 79]. They used a configuration in

which the optical tweezers pushed particles into an oil-water interface from the water phase. The water phase was positioned below a oil interface as illustrated in fig. 2.3c. The particle's vertical position was then tracked using holography. In this way, they were able to establish that particles exhibit a logarithmic relaxation into the interface. The vertical configuration allows for a completely flat interface, which can be advantageous, since accounting for the effects caused by curved surfaces can be difficult. However, imaging through the interface makes it challenging to discern exactly where the interface is. This configuration also makes it challenging to use the tweezers to measure and apply forces to particles during the adsorption, since reflection of the laser from the interface may affect the particle, and optical tweezers are less stiff along the z direction.

In these applications optical tweezers strength lies primarily in their ability to manipulate particles, rather than their force measurement, since the attachments too the interface are generally stronger than what a tweezers can achieve [80]. Nevertheless, as a non-contact technique with high resolution, optical tweezers are likely to play an increasingly important role in this field. In Paper III we make use of a different configuration to study particle adsorption in which the particles are pushed into microbubbles, offering direct visualization of the adsorption process.

Chapter 3

The SmartTrap system

Toward the end of the 1990s, optical tweezers became increasingly common in laboratories around the world as more and more laboratories learned how to use the techniques involved. Several breakthroughs were made, such as the first DNA pulling experiment and investigations of kinesin stepping [48,81]. One of the leading groups in the field of single-molecule studies with optical tweezers was, and still is, that of Carlos Bustamante. Steven B Smith, engineer in that group, and Carlos together had the idea of miniaturizing the system they had used for the DNA experiment. This became the MiniTweezers, an optical tweezers small enough to fit in a fridge. The instrument, illustrated in fig. 3.1, was quickly adopted by groups around the world, and since then around 50 instruments have been produced, many of which are still in use today. To mention a few example use cases from our collaborators; the lab of Felix Ritort has several MiniTweezers instruments and has been using them to investigate things like fluctuation theorems, free energies and binding energies of nucleic acids [82–84]. Geographically closer to our lab the group of Fredrick Westerlund and Marcus Wilhelmson have used it to study DNA hairpins [85, 86].

Working on the principle "if it is not broken, don't fix it", the original design and electronics are still (to our knowledge) used exclusively. When I started my PhD, this was starting to become a bit of a problem. It is increasingly difficult to acquire the necessary components for constructing new instruments, for instance the motors were discontinued in 2008. Also, being limited by the technology of its time, the instrument is starting to become outdated in terms of capabilities.

This was the background to the SmartTrap project, to reinvigorate the

MiniTweezers systems with new electronics, software, and minor hardware updates to breathe new life into the many MiniTweezers instruments around the world. In this way, we could address the shortcomings of the original design, while in the process also obtaining a cutting-edge instrument well suited for experiments ranging from single-molecule force spectroscopy to particle-particle interactions, and particle characterization.

Once our updated instrument had been constructed, we realized that the fact that we could control the entire system from our computer gave us several new opportunities to streamline our workflows. This initially led to experiments being performed remotely from the comfort of an office and in the company of a cup of coffee, but eventually enabled us to take it one step further and have the instrument perform our experiments autonomously. In this chapter, I outline how the SmartTrap system works, how to use it, and the differences between it and the older MiniTweezers. However, the algorithms used for automation are left for the final chapter of this thesis.

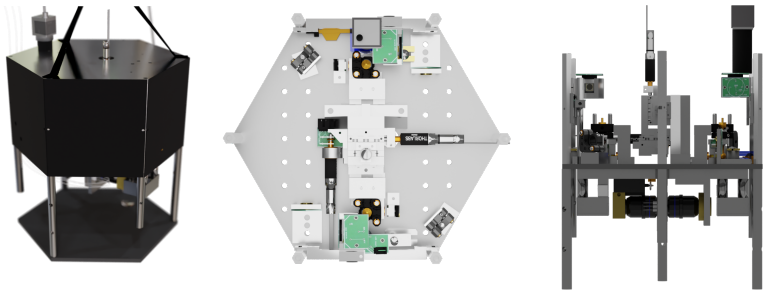

Figure 3.1: **The MiniTweezers instrument.** 3D model of the MiniTweezers viewed from the side with side panels (leftmost image), as well as from the top and side with the side panels and internal cables removed for better clarity. The instrument is ca 30 cm in diameter.

3.1 Experiments in the MiniTweezers system

To understand the MiniTweezers system, it helps to take the perspective of someone working in biophysics and who uses it on a daily basis. We therefore start by describing how experiments are performed. In particular, we focus on single-molecule force spectroscopy experiments, which allow for studying processes such as protein folding and unfolding, DNA dynamics

and molecular motors [8, 9, 53]. These experiments are further described in section 2.1, and it is for this type of measurement that the instrument was originally designed. Single-molecule experiments require the ability to manipulate at least one particle, while also being able to measure forces and distances. Beyond this, there are additional features of a system that are highly desirable, since they make experiments easier to perform, such as a reliable microfluidics system, an easy-to-use interface, and some pre-prepared pulling protocols.

Experiments in the MiniTweezers are performed in a custom microfluidics chamber. The standard chamber design is shown in fig. 3.2. The chambers are handmade by sandwiching two sheets of parafilm between two microscope slides made of glass. The parafilm is cut beforehand using a laser cutter to create the channels, and in one of the glass slides holes have been drilled for inlets and outlets. Importantly, the MiniTweezers has only one optical trap and therefore makes use of a micropipette, positioned in the center of the chamber, to hold one of the microparticles, see fig. 3.2. It is quite easy to adjust the chamber design. For instance, to perform the liquid-liquid interface adsorption experiments in Paper III, the design was altered to better allow for using the micropipette to create dodecane droplets by removing the outer channels and increasing the size of the opening in the micropipette.

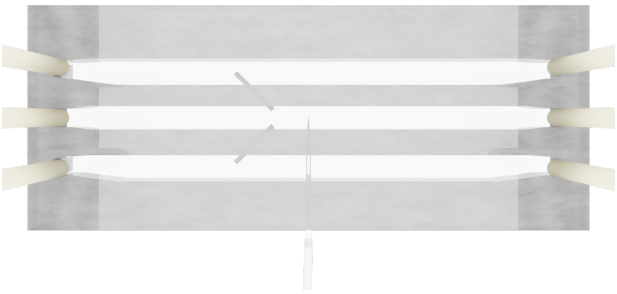

Figure 3.2: **3D model depicting the microfluidics chamber of the MiniTweezers.** There are 3 channels in the chamber, the top and bottom are used to supply particles and the central channel is used to perform the experiments. The bottom and top channels are connected to the central one with microcapillaries.

After having installed a microfluidics chamber with the corresponding

tubing, there are a few steps that need to be taken before an experiment can be performed to prepare the instrument. The zero levels of the force and position detectors are set to account for any slight misalignment. It is also advisable to save the motor encoder positions of the outlets of the capillaries in the central chamber as well as the pipette to avoid having to look for these after replacing a particle. With these steps performed, the system is ready for operation. A typical single-molecule experiment in the MiniTweezers system involves the following steps

1. A streptadavin coated particle is trapped
2. The particle is brought to the micropipette
3. The particle is placed in the micropipette, held there firmly by suction
4. An antidigoxigenin coated particle is trapped
5. The particle is brought to the particle in the pipette
6. The particles are brought together and pulled apart
7. The user looks for a force-distance curve resembling the molecule they are investigating
8. A pulling protocol is executed while forces and distances are measured

The above describes a typical procedure. However, it could easily be adapted to other experiments which can be performed in the MiniTweezers, such as hopping of a molecule between folded and unfolded states [87].

3.2 Optical system of the MiniTweezers

The MiniTweezers makes use of a counterpropagating optical tweezers design. That is, it uses two lasers to form a single optical trap, see fig. 3.3. There are several advantages to this. The scattering forces of the two lasers cancel out, creating a highly stable optical trap. Also, and perhaps most importantly, it allows for direct force measurement by monitoring the momentum change of the trapping lasers. This has the great advantage that once the system is calibrated the force acting on any trapped object can be calculated directly from the deviation of the lasers from their equilibrium positions, assuming that all light passing through the trapped object is collected. An assumption which holds true for most particles used in experiments with the MiniTweezers. In the MiniTweezers, the laser momentum change is measured using two PSDs, one per laser as shown in fig. 3.3.

Counterpropagating tweezers also come with drawbacks compared to single laser systems; they are more challenging to construct and align since they have two lasers, which roughly double the optics and electronics needed specifically for the lasers. It also means that it is necessary to align the lasers very accurately in 3D for a stable trap, ideally the two foci should perfectly overlap. This is especially important for small particles since these have a greater risk of the two foci being so far apart that both lasers may not focus inside the particle leading to unstable trapping. This is the main reason the system may struggle with trapping of particles smaller than 0.5 µm.

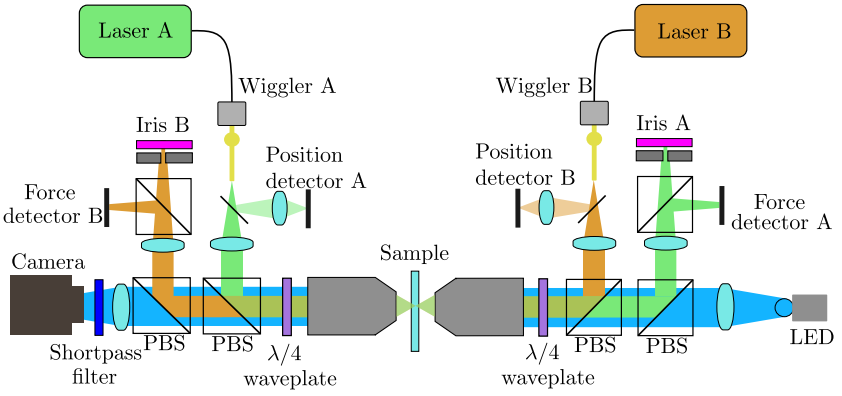

Figure 3.3: **Optical schematics of the MiniTweezers system.** The two lasers follow equivalent but mirrored paths. The lasers are first passed through the wiggler, which is used to move them dynamically. Next a small proportion is focused on the position detectors while most of the light is collimated and sent into the back aperture of the objectives. After passing through the sample the lasers are again focused this time on a second PSD (force detector) and some of it is focused on a photodiode with an iris in front. The photodiode is used for measurement of the force along the z-axis. PBS is short for polarizing beam splitter. Reproduced from Paper II.

Beyond the force measurement the system also incorporates position measurements of the lasers. Like the force measurement the actual position signal is sampled using one PSD per laser. These are placed before the lasers enter the sample and just a small portion (on the order of 8% of the light) is directed to them, see fig. 3.3. In the SmartTrap system these can be calibrated automatically with the camera, a routine moves a trapped particle in a grid pattern while tracking the position and recording the position

PSD readings. However, with the introduction of the digital camera the position recording is less important in the SmartTrap compared to in the MiniTweezers. The camera provides the true particle position, rather than the laser position, the latter needs to be calibrated to retrieve the particle position which is what is often needed for analysis of experiments.

The last important part of the optics of the MiniTweezers is the imaging of the sample. This is performed using a standard brightfield configuration as shown in fig. 3.3. As can be seen the path of the illumination pass through several different beam-splitters. All of these contribute to the illumination losing power, which makes achieving high intensities required for high-speed recording (with the camera) challenging. Not included in the schematics is a retro-reflector placed at the bottom of the instrument straight underneath the camera. With the retro-reflector installed, both of the lasers are visible in the camera, which is used for alignment.

3.3 From MiniTweezers to SmartTrap

Technology has advanced significantly since the MiniTweezers was originally designed, especially in terms of computing capabilities. This is why when we decided to update the MiniTweezers we focused on the electronics and the software. Microcontrollers today are smaller, faster and more powerful than they were two decades ago. Similarly, computers and digital cameras have advanced significantly, which has spread the use of digital video microscopy as a means of analysis. This has left the original MiniTweezers control system outdated, being overly complex and slow by today's standards, while also relying heavily on manual operation of different components (e.g. syringes for fluidics control). A prime example of this complexity is that the original controller required five different microprocessors to handle readings of the sensors and communication with the motors. Naturally, having a controller with five different processors makes the system very complex. In order to achieve a smooth operation of the user interface, the software needed to be highly optimized, which meant that customizing it for a certain computer operating system was necessary. This in turn meant users were practically forced to use only computers with that specific operating system. Still, the amount of work required to design a high-performance system such as the MiniTweezers, is not to be underestimated. This is why any half-hearted attempt at redesigning it would likely have yielded a system inferior to the original. Several aspects of it were well optimized also by modern standards, such as the force measurement, and remain high performance today.

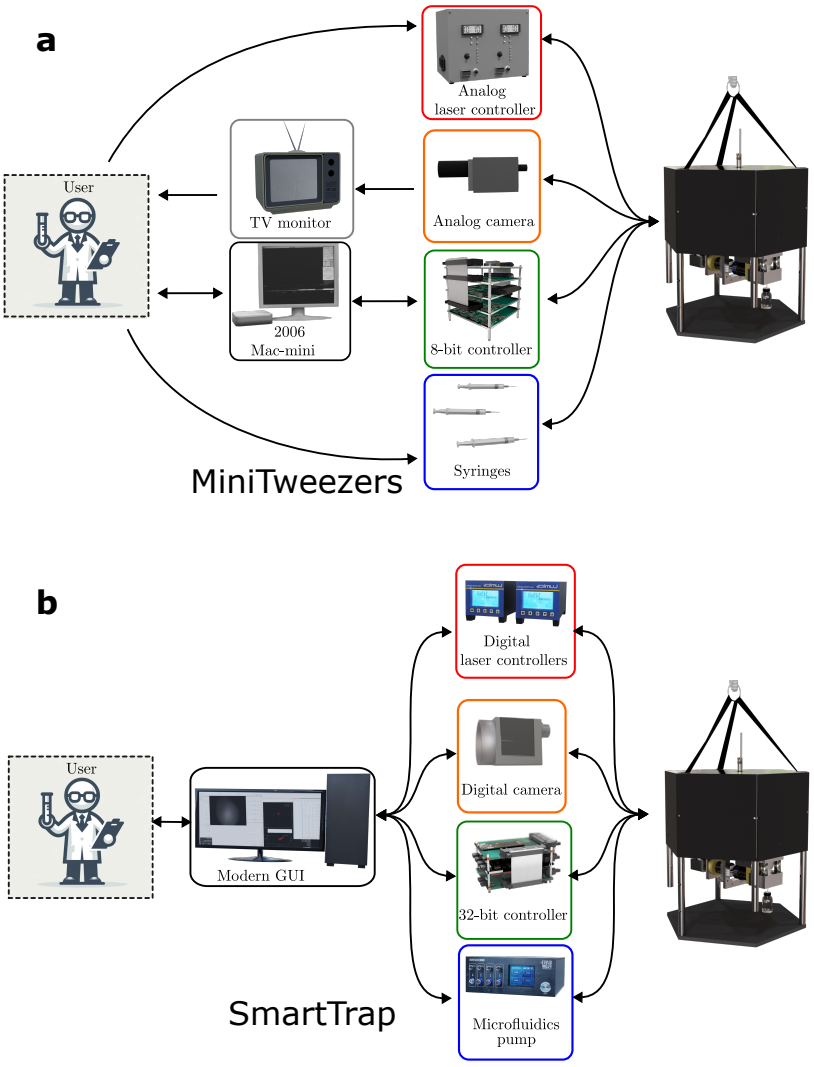

Figure 3.4: **Comparison of the new and the old MiniTweezers systems**. **a** In the old MiniTweezers system the user interfaced the system via a variety of different means. The camera was connected to a TV monitor, separate from the instrument itself and both particles and buffer were ejected into the instrument manually using syringes. Motors and laser positions were controlled from a Mac mini computer which also monitored the forces. **b** The new SmartTrap system lets the user control and monitor everything from a single interface.

The new system aims at addressing these shortcomings and simplifying the operation for users, as illustrated in fig. 3.4. Key to this were both the new controller and the new user interface. The new interface incorporates all the different control and monitoring systems used for the instrument into a single software application. This comes with two major advantages: first, it is easier for the user to only have to pay attention to a single software; second, it allows for more computerized feedback, and feedback between a larger range of different actuators and sensors. For instance, one can now have feedback between the camera and the pump, so that the pump, which pushes particles into the system, turns off immediately once a particle becomes visible, reducing the risk of double trapping particles.

3.4 Electronics controller

The instrument contains multiple photosensors (four PSDs and two photodiodes) and actuators (three servomotors and four piezos). These need to be read and controlled, respectively, at high speed. The role of the electronics controller is to communicate between the host computer and these sensors and actuators of the instrument, as illustrated in fig. 3.5. The controller also provides fast feedback for certain protocols. It consists of three separate printed circuit boards (PCBs) connected by ribbon cables. During my PhD I revised the design of the boards multiple times and now each board hosts a separate part of the electronics.

The first board hosts the microcontroller, a small programmable processor used to communicate with the computer. It also handles the digital signals on the controller, how this is done is outlined in section 3.4. Instead of using five different microprocessors, as in the old MiniTweezers, this board uses a single more powerful one. This not only simplifies the design massively but, since the processor is much faster, it also allows for greater sampling rates, reduced latency for feedback and simplified firmware programming. The microcontroller used is an Arduino Portenta H7 which is relatively powerful, easy to interface with and program while also being readily available.

The second board is used to read the photosensors. The signals coming directly from these sensors are rather low power so they are first amplified on the circuit board, in two stages, to be in the range of ca 1 V in amplitude before being sent to an analog-to-digital converter (ADC) which is then interfaced by the microcontroller.

The last board handles the actuators of the system, four piezos (two

for each laser) and three dc servo motors (for moving the sample in each axis). The piezos are driven by high voltage amplifiers capable of delivering up to 150 V and are controlled by two dual-channel (one channel per piezo actuator) digital-analog-converters (DACs). The motors are driven by pulse-width-modulated (PWM) signals which are amplified using a motor driver circuit. The motor driver circuit is also used for choosing the movement direction of the motors. Lastly, the board also passes through relevant signals to the microcontroller.

The controller has a two-way USB serial communication to the host computer, sending the various sensor readings to the host and receiving commands to execute, e.g., moving the sample with the motors or the lasers with the piezos. Since there is a fair bit of latency when communicating with the host computer some feedback protocols, such as the "autoalign" which keeps the two lasers at the same position on trapped particles, are run directly on the controller offering superior response times on the order of 0.1 ms.

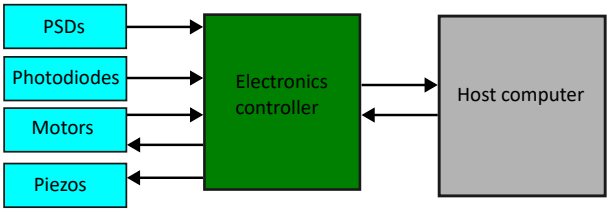

Figure 3.5: **Illustration of the role of the electronics controller.** The controller is responsible for converting electronic signals, in the form of voltages, from the various sensors to digital signals that are sent to the host computer. It also powers the motors moving the sample and the piezo actuators used in the wigglers to move the lasers inside the sample.

The new electronics controller is designed to be "plug-and-play" for existing users of the instrument. This means that they can replace their old controller with the new one by just moving the cables from the old one to the new one and connecting it to their computer. This offers an easy pathway for people to use it further into the future. With a sampling rate of ca 15 kHz (simultaneously across all sensor channels) it vastly outperforms the previous implementation in terms of data transfer speed, allowing the system to investigate also phenomena that happen on the sub-millisecond timescale. If even higher sampling rates are needed, external pin connectors on the controller can be used to connect it directly to an external oscillo-

scope.

Microcontroller firmware

There is a custom firmware running on the microcontroller which has been designed specifically for the SmartTrap system. Similarly to the interface described in section 3.5, the firmware runs a continuous loop. The loop is initiated when the controller is turned on. During the initiation, parameters such as which pins are used for output and which for input are set and communication with the host computer is started. If communication is dropped for any reason the microcontroller will continuously try to reconnect.

The main loop handles regular communications with the host computer and steers the piezo actuators. It checks when sufficient number of samples have been collected to send to the host computer. The loop is carefully balanced so that each iteration of it should take roughly the same time to execute. This means, for instance, that it does not read signals from the computer immediately after sending data, since doing so could block the timed sampling of the detectors. This reduces the risk of interference with the sampling, which is essential for stable operation.

Sampling of the various detectors is executed once every 64 µs. This sampling is triggered by a software trigger, meaning that once the internal clock of the microcontroller has detected that 64 µs has passed it will call the sampling function. The sampling function reads the A and B channels in parallel going through the different signals in order and putting them in a 512 byte array which when full is sent to the host computer via the USB protocol.

The microcontroller does not sample sensors directly itself. Instead it reads the values using a 16-channel 16-bit analog digital converter (ADC). This is interfaced via a parallel interface, meaning that each bit of the 16-bit number is read as a separate digital signal. A single pin on the ADC is connected to each of the amplified signals corresponding to the x,y and sum signals of the four PSD detectors as well as the power reading of the two photodiodes (which are used to determine the force along z). Due to limitations of the microcontroller it cannot use the Serial Peripheral Interface (SPI) communication in combination with the software timer, even though it is both faster and more flexible than the parallel interface and there are pins available on the microcontroller for that.

The smart trap system makes use of DC servo motors, specifically Thorlabs Z606 Motorized Actuators to move the sample stage. The speed of these are controlled using a pulse width modulated (PWM) signal. To en-

sure consistent speeds a position-derivative (PD) algorithm is used to adapt the PWM duty cycle. This is needed since the resistance when moving along different axis may not be the same. The motors have encoders that are used to determine when they have moved by sending a small pulse which triggers a counter on the microcontroller. These are used to calculate both the speed and position of the motors and depending on the movement direction the counters either increase or decrease.

The piezos, which steer the wigglers, are controlled using two digital analog converters (DACs), one per laser. The microcontroller communicates with the DACs using SPI communication. The voltages applied to the piezos regulate their extension, which in turn steers the lasers. The microcontroller communicates with the piezos at a rate of ca 7 kHz. The various movement protocols used in force spectroscopy are run on the microcontroller. These are called from the main loop. New protocols can be added with ease by implementing a new feedback function steering the lasers using the readings from the various photosensors to provide fast feedback.

3.5 User interface

Users operate the SmartTrap system using a custom graphical user interface (GUI) developed specifically for it. It is entirely graphical and written in Python, making it easy to maintain, use, and possible to run on all modern computers. The interface handles communication with the various instrument controllers and the camera. Being open source means that other users can, in principle, use it directly by downloading it from the GitHub repository [88].

The various controllers, or actuators, which are interfaced through the GUI (e.g. microfluidics controller, laser controller) are each assigned to a custom widget. A widget is a small container which show up as a small window to the user. This can then be moved around, resized and docked to allow the user to customize the interface to his or her own liking. These are visible in fig. 3.6 as rectangles.

Several key interactions are controlled with the computer mouse. For example, clicking and dragging moves the motors, while holding down the scroll wheel and dragging adjusts the focus along the z-axis. Users can select which tool to use by either clicking its icon or using a keyboard shortcut. Visual feedback is provided on screen, for instance a red box appears when selecting an area to zoom into. These tools are easily extended. For example, users can quickly implement functionality to select and save images of

Figure 3.6: **A screenshot showing the graphical user interface.** The central panel shows the camera feed. The user has the option to view, in real-time, the network predictions. These are indicated directly in the camera feed with a green bounding box encompassing the micropipette and a circle the particles. All the various parts of the system can be controlled manually. Each component is grouped into a specific widget which can be freely moved. To the left are laser controls, including positioning and autoalign feedback.

specific particles, using the provided interfaces and the network's predictions to center the images.

On top of offering control of the instrument, the software also allows for flexible monitoring of the various signals. This is achieved by a real-time plotting tool, built on the PyQtGraph package [89], which can display any of the different signals, plotting them in real time as shown in fig. 3.7. Such as the forces acting on the trapped particle, the position of the lasers and the tracked position of the particle. The user can open multiple windows, e.g. plotting the force as function of time in one window and as function of particle position in another. The plotting tool also offers some basic analysis tools which can be applied directly to the graphs while they are being plotted such as a Fourier transform and a rolling average. Especially averaging is useful to *average out* thermal fluctuations in real-time for easier monitoring. The plotting windows also allow users to export graphs directly, reducing the need to code when visualizing the data.

A range of keyboard shortcuts helps streamline manual operation. Each shortcut can be viewed by hovering the mouse over its corresponding button. The interface also allows users to see what the neural networks are predicting (as shown in fig. 3.6). For example, the color of the particles changes depending on their state: red when trapped, green when inside the pipette, and blue when moving freely. The force applied to each particle is shown in real time as an arrow drawn on the image, with its length proportional to the force magnitude and direction. These features help users quickly understand the system's current state, such as whether a molecule is attached during an experiment.

Automation algorithms are also managed directly from the interface. Users can activate or deactivate any of the available autonomous protocols or choose to enable only specific subroutines, such as particle trapping or pipette alignment. This flexibility is particularly helpful for troubleshooting or focusing on a single step of an experiment. When automation is running, the interface shows which step is currently being performed, keeping the user informed in real time.

3.5.1 Back end of the user interface

Several technical challenges had to be overcome to ensure smooth and stable operation of the system. Most of these solutions are not directly visible to the user, but they are crucial for reliable performance. The back-end operates in a continuous loop, constantly acquiring data and monitoring signals. It also manages communication with external devices such as the

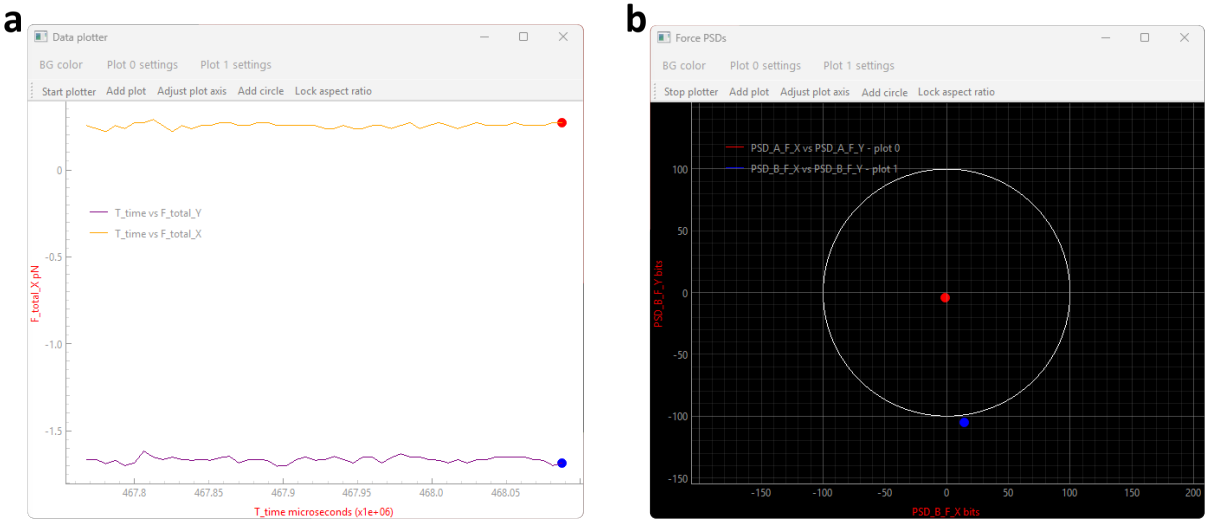

Figure 3.7: **Screenshots showing examples of live plots from the interface. a** The force along X and along Y as function of time. **b** The current force readings of laser A and B. Both axis are in pN meaning that the position of the circles should be interpreted as the force applied by the corresponding laser on the trapped particle.

camera, laser controllers, and microfluidic pumps. Communication with external devices can sometimes cause the program to become unresponsive while it waits for a device to respond. Although these tasks are generally not computationally demanding, they are limited by input/output (I/O) speeds.

To prevent the interface, and the entire program, from freezing, the software uses multiple threads and processes. Threads are especially useful in Python for handling I/O-bound tasks. At a minimum, the program uses five threads and one extra process, and more if all plotting and sub-units are enabled. These are outlined in table 3.1. Threads in Python are executed by the same physical computer core as the main code and are thus well suited for I/O-bound tasks, but not for computationally heavy tasks. For computationally demanding tasks, one can instead in Python make use of separate processes, which, unlike threads, run on a separate core on the computer. The back-end uses a separate process for reading and sorting the data that comes from the instrument controller. Using multiple threads and processes makes the program more complex than a single-threaded application, but this approach proved necessary to maintain responsiveness and stability. Importantly, the back-end code is designed to be reusable for other interfaces or applications.

Generalizability of the software

Even though the software has been tailored to the SmartTrap system, it is designed in such a way as to be easy to transfer to other systems. This is achieved by using software interfaces that provide blueprints detailing which functions need to be implemented for the system to work. The motor controller class, for instance, needs to have functions for moving to a pre-specified position, reading the current position and moving at a specified speed and direction. As long as these functions are implemented, the software can use the motor controller. Meaning that if a user replaces the motors and controllers of the system smart trap system, by just implementing their own motor controller class, all functionality will remain. Similarly, the camera only needs a few functions, such as one for capturing frames and setting the field of view, and can easily be replaced, as we did in fact do for Paper III. There are also interfaces for the real-time tracking, microfluidics pumps, laser controllers and data collection.

Looking further ahead, it is our hope that this will lead to other groups adapting and building on, the software. This could lead to more researchers trying automation. There will of course still be a need to adapt some of

Table 3.1: **The different threads used by the SmartTrap system.** By using multiple different threads the program limits influence of both I/O-bound tasks and computationally demanding tasks on the operation of the system.

Thread or process	**Function**
Main GUI	Runs the main GUI and shows the camera view to the user.
Camera	Continually captures images from the camera. Also updates camera settings (e.g. exposure time) when needed.
Video recording	Records videos from captured frames.
Instrument communication	Continually sends data to and from the instrument, placing the recorded data in a queue. Runs in a separate process.
Data preprocessing	Reads data from the data queue and sorts it based on sensor. Also calculates forces and laser position.
Plotting	Plots data in real-time in a separate window. Can be multiple different windows (each with a separate thread) and are started from the main GUI.
Automation	Handles the autonomous procedures and performs the real-time tracking of particles and pipette.
Microfluidics	Communicates with the microfluidics pump. Regularly checks the current pressures.

the automation routines, but the amount of extra work required will be substantially smaller.

Chapter 4

Automation of optical tweezers

With the rise of AI, and in particular large language models (LLMs), the trend of automating work has gained renewed speed recently, which, as we note in Paper I, has been followed by a massive rise in the number of papers published in the field. The reason for this rise is in large part the hope that AI can replace human labor in a range of tasks, thus greatly reducing the cost of services. This trend is also starting to reach the laboratory with AI models being used in, for instance, protein design and experimental design [90, 91]. However, the challenges faced when automating an experimental procedure in a research lab are often very different from those faced when developing tools like LLMs which aim to replace standard everyday tasks such as answering emails or customer questions. One of the largest differences is that the amount of training data available in a laboratory setting is often minuscule by comparison. This means that an approach based solely on machine learning is often unfeasible [92, 93].

Automation has reached less far in several aspects of lab work, so relatively easy tasks may not yet have been automated, although the techniques required to do so are readily available. In this chapter we take a look at the techniques used when automating the SmartTrap system, and when possible, a more general overview is given so as to provide directly useful insights also to people aiming to automate their own related tasks like smart microscopy, magnetic tweezers or AFM. The focus is primarily on more advanced aspects of automation, meaning those enabled by advanced image analysis or the integration of multiple different components.

4.1 The case for automation in biophysics

There are multiple reasons to automate procedures, the primary one being increased productivity as measured in output per human working hour, but also, and perhaps more importantly, increased repeatability and quality control. Starting with the increased productivity, having an instrument running for extended periods of time on its own frees up researcher time and allows for gathering larger datasets. This is important in biophysics in particular since results from the laboratory, as well as theoretical models, are increasingly dependent on large amounts of data. A prime example is that of AlphaFold which, when trained on 170,000 protein structures, was able to accurately predict different protein structures [94]. In the case of optical tweezers, throughput is also believed to be the key to the adoption by the pharmaceutical industry [54].

Reproducibility of results is absolutely central in science, yet it has long been an issue with many replication attempts failing [95]. Having automated and standardized procedures could help scientists compare and reproduce results, both from different groups and performed with slightly different parameters, e.g. temperature or cell lines, increasing reproducibility [96]. Repeatability is key for enabling researchers to uncover heterogeneity in results. If experiments are performed slightly differently each time, due to manual operation, then it is difficult to tell which part of the variation in results comes from the execution and which from the intrinsic heterogeneity of the processes studied.

A third potential benefit is that automation can unlock completely new applications that are not possible without some sort of intelligent, and fast, feedback which is unattainable with manual operation. A simple example of this is the "autoalign" procedure described in Section 3.4 above. This operates much faster than a human can and enables fast movement of our counterpropagating trap. It is easy to imagine other smart applications in which the system automatically responds rapidly. For instance, detecting misfolding in a protein experiment and responding to this by bringing a second protein close to see if it binds specifically to the misfolded protein.

With this in mind, it is natural to ask when not to automate, or why automation is not more widespread. Again, there are multiple reasons and they differ between applications. There is little literature discussing why automation is not more widespread. Focusing on experimental sciences in academia, and drawing from my own experience, one reason is that it may take longer to automate a procedure than to manually acquire the required data. We believed this to be the case for the work presented in Paper III. Of-

tentimes the skills required to implement automation procedures differ from those needed to prepare and perform experiments. The former being typical research tasks, requiring knowledge of chemistry, biology or physics while the latter is more technical, needing experience in electronics, programming and mechanical design.

However, now that there is a freely available implementation of several experimental procedures (SmartTrap GitHub [88]), this cost-benefit calculation has changed and the effort needed has been reduced. For many experiments going forward, it is likely that several (or all), steps will be automated. Furthermore, also when not automating an entire procedure, more advanced assistants could help increase the throughput of manually performed experiments by, for instance, helping with alignment or real-time analysis.

4.2 Literature on optical tweezers automation

There has been some work on automating various optical tweezers applications and protocols prior to our work, but as concluded in Paper I these works are few and still only rarely use machine learning. Some small parts of experimental procedures in optical tweezers have long been automated, such as pulling protocols used in the MiniTweezers, but these are mostly very simple and generally need to be programmed for each experiment. Nonetheless, there are several noteworthy works making use of more advanced automation.

One of the first optical tweezers applications to be automated were particle sorting, or perhaps more accurately particle selection. There are multiple different sorting methods which rely on optical forces and they can be broadly split into active and passive sorting algorithms [98]. Passive algorithms make use of different response to optical fields for different particles which gives rise to different forces acting on them which enables sorting. These methods often have relatively large throughput, but are less flexible when it comes to the sorting criteria. By contrast, active methods require a choice by the operator (or system) based on a different criteria, such as shape or refractive index, to separate particles as illustrated in fig. 4.1 a. An early example of this was the combination of microfluidics with image analysis to sort cells by type [99], while some more recent methods rely on deep learning for classification [100–102]. Active sorting makes use of optical *tweezers*, not just optical forces. Still, even though throughput is modest compared to passive methods, the complex criteria that can be employed makes active sorting highly flexible.

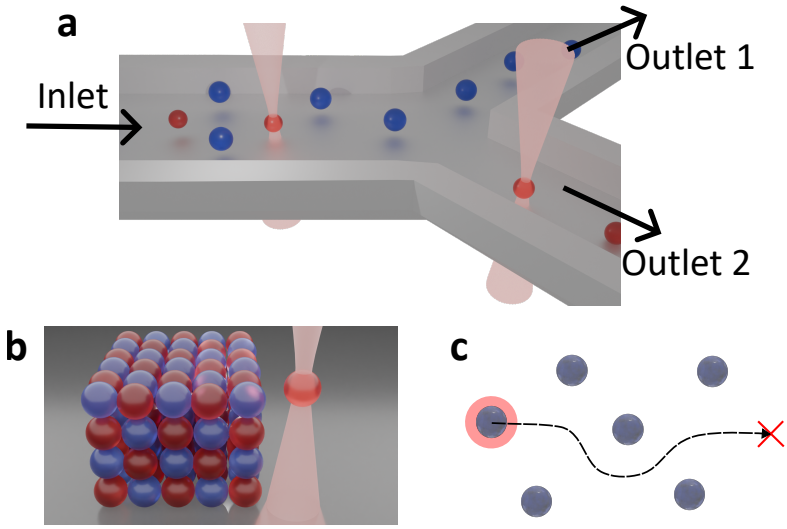

Figure 4.1: **Illustration of automation of optical tweezers found in the literature.** **a** Sorting of particles (or cells) has previously been performed with optical tweezers. By incorporating image analysis and microfluidics particles can be actively sorted with optical tweezers based on different criteria (shape, size, fluorescence, etc). **b** Assembly of particles. Complex 3D structures can be assembled using optical tweezers and particles that adhere to one another. **c** Navigation through complex environments. By tracking the position of multiple particles optically trapped particles can be moved without colliding with obstacles [97].

Optical tweezers have been automated to assemble microcrystals from microparticles as illustrated in fig. 4.1 b. In practice one or several particles are trapped by the tweezers and then brought to the crystal where they are attached to it, building complex structures particle by particle. In my opinion, this is the most advanced application to be automated to date (not counting the SmartTrap) since it requires both positioning and trapping of multiple particles. Primarily two different approaches to attaching particles have been used, curing of photocurable prepolymer between the particles and attachment using biotin-streptavidin binding (particles with two different types of coatings) [103, 104]. These methods have been proposed for assembling photonic crystals. While they offer a highly versatile means of particle assembly, their throughput, also in automated implementations, remains lower than that of other nanofabrication techniques. As a result, they are more likely to find applications in prototyping rather than large-scale manufacturing.

There has been progress in applying machine learning in the steering of the tweezers, a prime recent example is [97] in which they use reinforcement learning to navigate a crowded environment with a trapped particle, illustrated in fig. 4.1 c. Their goal is to move a particle to a specific location without the trap overlapping with other particles. It is highly interesting in that it makes use of reinforcement learning to directly control the tweezers and achieve a quite complex task. Also, it is worth noting that the system was trained a simulated environment and could thus relatively easily be adapted to other similar tasks (e.g. avoiding actively moving obstacles such as bacteria). However, for this particular case, there are good and widely available classical algorithms such as the A-star algorithm [105] which is commonly used in robotics and video games as an efficient method for navigating a complex environment. Still, being a quite fundamental task in optical tweezers experiments, it may very well see use as part of other automation applications.

In summary, several components of optical tweezers systems have been automated. However, the number of fully automated applications in the field remains limited, and their adoption is largely confined to the laboratories that originally developed them. To date, there has been no systematic review of why this is the case for optical tweezers in particular. However, many of the obstacles are similar to those encountered when automating biological experiments more broadly, allowing us to make some educated guesses about the underlying factors. As is often the case, the issue likely reduces to a cost–benefit calculation. Most laboratories lack the necessary expertise in programming, image analysis, and electronics to implement au-

tomation themselves. Thus the cost of automation is much higher than the cost of manually performing the experiments. Also, many users do not build their own tweezers setups and may therefore have limited control over them. The rarity of automation may also reinforce the perception that it is prohibitively difficult, although in practice, the challenge is only for the first experiment. Similarly, because experimental protocols differ substantially between studies, automation may be perceived as requiring a near, complete reinvention for each new experiment, further limiting its appeal. Finally, many optical tweezers experiments do not require large amounts of data, which reduces the benefits of automation.

4.3 Building an autonomous system

As noted in Paper II, when building an autonomous (optical tweezers) system three key components are needed: firstly a system which can be automated; second sophisticated data analysis running in real time; and lastly automation algorithms based on real-time feedback.

4.3.1 Designing an automation-ready instrument

The key for building an automation-ready system, such as the SmartTrap, is to ensure that it is designed in such a way that all components needed to perform multiple consecutive experiments can be operated using a computer. In our case, we made sure that all proprietary controllers were directly compatible with the Python programming language. This is convenient, since Python is widely used in machine learning which in turn is used heavily in the image analysis, but direct Python integration is not strictly necessary. As long as the different subsystems are controllable by a computer one can generally make them work with almost any program by putting in a bit more work to create a compatibility layer, e.g. Python programs can call on LabVIEW scripts and vice versa.

I highly recommend starting with making sure that multiple experiments can be performed consecutively and remotely, without needing to enter the lab. This ensures that the system is in principle possible to use for autonomous experiments. By doing this before starting with the programming one reduces the risk of needing to physically redesign the system at a later stage and then also needing to reprogram it.

Some parts of a system may be challenging to control digitally (e.g., alignment mirrors in our case), but the more the better and it is worth

keeping in mind that even just automating parts of a procedure can lead to significant productivity gains.

4.3.2 Advanced analysis for real-time applications

The data analysis is needed to make sense of the sensor readings, and in the case of optical tweezers, it is the camera and therefore image analysis which is most crucial. This is needed to determine where particles are, and if one is trapped. Importantly, it is not only the camera that is used. For instance, the force readings are necessary to understand if a molecule has attached during an experiment.

The requirements of real-time analysis differ somewhat from those of analyzing previously acquired data. Firstly, high speed is needed to provide feedback quickly. What counts as 'fast enough' varies between applications, but as a rule of thumb it should be below 0.1 s, comparable to the reaction time of a human operator. Crucially, it is the latency that must be minimized. In non–real-time machine learning, data is typically processed in batches—for example, a network may analyze hundreds or thousands of images simultaneously. This approach allows very high throughput through massive parallelization. However, batch processing inherently increases latency. As an example; a system capable of analyzing 1000 consecutively captured images per second with a 1-second latency may be less effective for automation than one analyzing only 2 images per second but with a 0.5-second latency, since the latter can act on more recent data.

Second, the analysis needs to be robust to noise. Otherwise it will soon run into trouble when operating. For instance, a risk of 1% of missing a particle detection means that within just a few seconds the system is likely to think that it has lost a particle. In the SmartTrap this is overcome in part by looking at several detections and only if multiple consecutive predictions agree that a particle is missing acting on it.

However, a real-time analysis is not more demanding than a post aquisition analysis in all aspects. Oftentimes there is no need to analyze all the data in real-time for a real-time application, it can be saved for later. Again, taking the SmartTrap as an example, if the framerate of the camera exceeds that of the analysis then not all frames are analyzed. Also, some precision can be sacrificed to achieve high speed and robustness. The real-time tracking in Paper II is a case in point here, it operates at ca 20 Hz with inferior precision compared to a U-Net. But, being much faster and less sensitive to particle size and focal position, means that it performs better than the U-Net for this application.

Looking forward, it is likely that machine learning will take an increasingly large role in the analysis, as we discussed in Paper I. It also seems likely that specialized hardware, such as FPGAs, will be used for some of the feedback algorithms to decrease the latency, which comes from sending data between different computing devices.

4.3.3 Automation algorithms

To automate advanced applications, equally sophisticated algorithms are required. In the simplest case, these algorithms follow a fixed protocol without feedback, so called *open-loop* control. For example, a particle might be moved at a constant speed between two predetermined positions without regard for whether it is trapped. In more complex scenarios, such as moving a trapped particle between other moving particles, more advanced algorithms are needed which make use of feedback signals in *closed-loop* control. These algorithms must react to events in real time, and they must do so quickly. For some problems, there are ready-made feedback algorithms, such as the proportional–integral–derivative (PID) control algorithm [106]. However, when there is a large range of possible actions, the challenge lies in deciding what to do in each specific situation, and often custom decision algorithms are needed.

We use the autonomous DNA pulling experiment as an example of what the decision process can look like, the flow of the algorithm is illustrated in fig. 4.2. The algorithm continuously returns to a standard position from which decisions are taken to follow one of four paths. Which path is followed depends on if there is a particle in the optical trap, and if there is one the pipette or not, as illustrated by the particles with question marks. The four different paths correspond to the four different possible outcomes of these two checks as outlined in table 4.1.

Table 4.1: Possible outcomes of the check in fig. 4.2 whether there is a particle trapped and one in the pipette. There are four possible outcomes of the check and therefore four different actions that may be taken.

Trapped	**Pipette**	**Action**
No	No	Collect SA particle
Yes	No	Put particle in pipette
No	Yes	Collect DNA particle
Yes	Yes	Initiate experiment

However, the algorithm is more complex than what fig. 4.2 gives the impression of. Many of the single steps are themselves feedback loops with decision processes. The algorithm used to trap a particle (once near the correct capillary opening) and the one used for attaching molecules are examples of this. The trapping algorithm is illustrated in fig. 4.3. The loop starts by checking if a particle is trapped, if that is the case, then it terminates. A particle is considered trapped if it is sufficiently close to the optical trap. If no particle is trapped, it checks if there are particles in view. If there is a flow from the capillary, this is turned off, and the instrument moves to trap the nearest particle. Thereafter, it returns to the starting point of the loop. If there are no particles in view the instrument will move back to the capillary opening (it may have moved away if a previous trapping attempt failed). Then it will turn on the flow of particles and return to the starting point of the loop.

These algorithms are run in the same loop as the tracking to avoid synchronization problems which could arise from acting on outdated data which would otherwise risk the system for instance moving twice the distance needed to trap a particle. This particle trapping algorithm is a typical example of a subroutine that can be re-used for different autonomous applications and which also with a slight change of parameters can be adapted for other purposes. In the red-blood cells experiment of Paper II, which was performed using only the main microfluidics chamber, the flow from the capillary was replaced with the flow of the main channel. By removing the optical trap from the system it can instead be used to keep a freely diffusing particle in the center of the screen.

There is a key difference when working with real-time systems compared to much of the programming performed in research, such as simulations and data analysis, namely that the programs must run continuously. This means data used to make decisions come in gradually as the program runs and all different data needed may not be available at the same time (e.g., may need to wait for the camera to take a picture even if the force is already measured). Furthermore, one needs to be able to safely cancel operations without stopping the entire program. Stopping at the wrong stage of a procedure may lead to damages, for instance by leaving the instrument turned on with high pressure or while trying to move the sample chamber towards the objectives. This is absolutely essential to take into account when programming an autonomous system which will continuously act based on its inputs.

Testing of systems that operate with physical systems is significantly more challenging than testing a system with purely digital inputs (e.g. a

pure simulation). This makes working with a system that will control a device operating in the real-world more challenging than developing an algorithm that runs in a purely simulated environment (e.g. a video game). Because of this, many choose to develop specific test environments purely for the purpose of testing their algorithms substituting real-world inputs. In the case of the MiniTweezers, developing a dedicated test environment was deemed too time consuming. Instead, various strategies were used to simplify development and testing. Essential for testing was to break the procedures into subroutines, as discussed before, each of which can be tested and optimized separately. This has the added advantage of making the subroutines (such as trapping and alignment) more reusable. It is also something that I can strongly recommend for anyone seeking to develop their own autonomous system. Also, drawing up a flowchart describing the algorithm, similar to fig. 4.2, can help giving an overview and identifying the various subroutines needed.

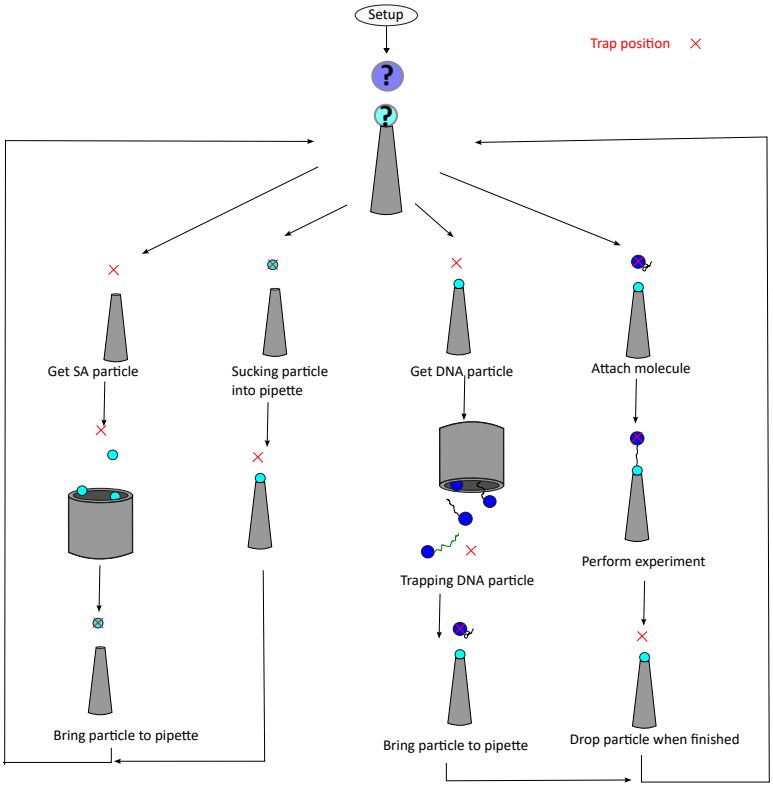

Figure 4.2: **Automation flow of a single-molecule experiment.** A simplified flow-chart describing the decision process in the autonomous experiment. After an initial configuration the system focuses the pipette and thereafter checks if there is a particle in the pipette and if there is one in the trap. There are four possible outcomes of these checks which results in four different actions; trap a SA particle, put the trapped particle in the pipette, trap a DNA particle and try to attach molecule. After each of these action paths have been finished the system reverts back to checking the pipette. **b**

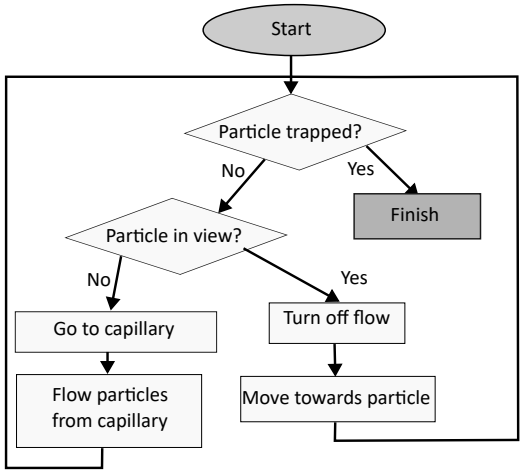

Figure 4.3: **Flow chart illustrating the algorithm used for trapping particles**. The algorithm starts by checking if a particle is trapped which is done by checking if there is a particle close enough to the optical trap. Next it will look for particles in view that are not trapped. If there are any, it turn off the flow of particles and will move towards the closest one in view before returning to the start state. If there are no particles in view it, will move towards the capillary and start the flow of particles. The loop finishes once a particle is trapped.

Chapter 5

Conclusions and outlook

During my PhD machine learning, and deep learning in particular, went from being applied in only a handful of niche problems to becoming a mainstream tool in research and technology. When Paper I was published, we predicted that deep learning would continue to find new applications in optical tweezers. This prediction seems to have been correct, not only are our own developments in Paper II an indication of this, but there are also several new works that apply machine learning to enhance optical tweezers experiments, for instance for counting and classification [100–102]. The rapid pace of progress suggests that this trend will continue.

In Paper II, we presented what might be the most advanced autonomous optical tweezers system developed to date. This system will only become more powerful over time, reducing the risk of experimental mishaps (such as lost particles), while further increasing throughput, reproducibility, and robustness. While obvious improvements can be made by boosting processing speed, tracking accuracy, and stage control, there are also hardware limitations that could be addressed. For instance, the reliance on a micropipette for fixing a reference particle is often problematic, requiring careful 3D alignment and being prone to clogging. Improvements here would simplify protocols considerably, for instance, by using a system with two optical traps.

On the software side, more sophisticated control algorithms could expand the range of feasible experiments and reduce the chance of costly mistakes. An open question is whether neural network–based controllers, such as deep reinforcement learning agents [107], could offer superior performance; however, I concluded that such an approach was not practical during my PhD

(largely due to the lack of an adequate simulation environment for training) the progress in reinforcement learning elsewhere suggests that, given sufficient resources, such an approach may indeed become viable in the near future. Especially considering that such agents have been able to master complex video games such as Minecraft and StarCraft II [108, 109]. For now, our modular automation framework, based on independent subroutines for trapping, alignment, and measurement initiation, etc, provides an efficient and flexible architecture. It allows new experimental protocols to be assembled rapidly from tested building blocks.

This modularity is already being used in collaborations to implement new autonomous protocols, particularly for studying protein folding and motor proteins, which will be a central part my colleague of Aarón Domenzain's PhD work. Another promising direction is to adapt these protocols to operate on other optical tweezers platforms, which could accelerate adoption across labs. Importantly, autonomous protocols may also facilitate industrial use of optical tweezers, where the major bottleneck is currently the challenge of collecting sufficiently large datasets for optical tweezers to be relevant [54]. This challenge is well known in single-molecule research, where the intrinsic heterogeneity of the systems means that robust conclusions often demand large datasets [49]. In this sense, automation is not just a convenience but a necessity for moving the field forward.

In Paper III, we turned to colloidal physics and introduced a novel approach for studying adsorption and desorption at liquid–liquid interfaces. The use of optical tweezers for analyzing colloidal interactions goes back a long way [70]. Our direct visualization of adsorption and desorption processes using force measurements was possible because of the particular design choices made in the SmartTrap system, especially the relatively low NA of the trapping lasers, which reduced interference with bubbles. A natural next step is to systematically vary parameters such as bubble size, ionic strength, and temperature to more fully map the adsorption dynamics. The discovery of reversible adsorption was particularly striking, and our choice to model it using a worm-like chain framework was motivated by the similarity of the measured curves to those observed in single-molecule experiments. This reversible attachment hints that aggregation in such systems may be reversible and relatively weak. However, it is worth noting that we are still working on the paper, so we need to be careful about drawing too far reaching conclusions.

From a methodological standpoint, these experiments also highlight the challenges that arise when developing entirely new measurement techniques. The extreme stickiness of the particles meant that automation was imprac-

tical at the time, but in retrospect, a partial automation—such as automatic estimation of bubble size and focus—would have improved reproducibility and throughput. Looking forward, combining advanced control with the ability to probe how a single particle responds to environmental changes (e.g. pH, salinity, or temperature) could open new avenues in colloidal science.

Finally, in Paper IV we addressed a central technical problem: how to reliably calibrate force measurements under non-ideal conditions. The methods we developed are particularly valuable for trapping particles that are difficult to observe directly, such as small fluorescent particles or molecules, and thus broaden the scope of conditions under which optical tweezers can yield meaningful results. This methodological advance is widely applicable and will help ensure that force spectroscopy remains useful even in experimentally challenging regimes.

Together, the four papers in this thesis showcase both the versatility, and the future potential, of optical tweezers. From automation to novel applications in colloidal science, to robust methods for calibration, the work points toward a future where optical tweezers are not only more powerful but also more accessible. The rise of automation will be central in bridging the gap between single-particle precision and large-scale ensemble studies, enabling optical tweezers to contribute meaningfully to fields as diverse as biophysics, materials science, and industrial research.

A common thread running through this thesis is the idea of scalability: of methods, of experiments, and of insight. Automation and machine learning promise to scale up the complexity and throughput of experiments; robust calibration extends the range of conditions where tweezers can be applied; and novel protocols expand the scientific questions that can be asked. These developments suggest that the next decades may see optical tweezers move from being a highly specialized tool to becoming broadly adopted also in practical applications and in more fields of research, and perhaps also in industry.

Acknowledgements

Many people have helped make the projects in this thesis possible. When I first started my PhD, Alessandro Magazzù taught me how to work in an optics lab and introduced me to the basics of optical tweezers. Together, Alessandro and I explored applying optical tweezers to particle correlation measurements.

Eventually, the work on the SmartTrap could begin. Isabel and Felix enabled us to test that our MiniTweezers were working by providing λ-DNA and anti-digoxigenin particles for our initial experiments. My brief visits to their lab gave me valuable experience, as well as the rare opportunity to discuss the system with people who use it daily and had assembled it themselves. Vinoth Sundar Rajan was absolutely central in teaching me the practical aspects of operating a MiniTweezers instrument. Both Antonio Ciarlo and Giuseppe Pesce also played key roles in getting the instrument to function properly. Anders Schenström deserves special mention for his assistance with countless orders of components, often requiring navigation through the complicated procurement rules of a public university. Antonio also deserves acknowledgment for providing the entire Softmatterlab with a steady supply of excellent Italian coffee—something that became increasingly important to me personally as the deadline of this thesis approached.

Steven Smith helped guide me in the right direction when assembling our MiniTweezers instrument and deciding how best to improve it. Carlos was central in writing the SmartTrap paper and gave me a strong foundation in single-molecule experiments more generally. I am confident that the collaboration we began will continue with Aarón Domenzain, who is now taking over operation of our SmartTrap system.

Giovanni—although the busiest person I know and highly skilled at delegating work—has always been quick to respond and has offered invaluable guidance throughout my PhD. He has taught me how to work independently and with increasing focus.

Lastly, I would like to thank the entire Softmatterlab and the Department of Physics at the University of Gothenburg for their support and for being such wonderful colleagues.

September 2, 2025
Martin Selin

Bibliography

[1] Henry Gray. Anatomy of the human body, volume 8. Lea & Febiger, 1878.

[2] Anton R Sobinov and Sliman J Bensmaia. The neural mechanisms of manual dexterity. Nature Reviews Neuroscience, 22(12):741–757, 2021.

[3] Richard Feynman. There's plenty of room at the bottom. In Feynman and computation, pages 63–76. CRC Press, 2018.

[4] Roland Glaser. Biophysics: An Introduction. Springer Science & Business Media, 2012.

[5] Jan Gieseler, Juan Ruben Gomez-Solano, Alessandro Magazzù, Isaac Pérez Castillo, Laura Pérez García, Marta Gironella-Torrent, Xavier Viader-Godoy, Felix Ritort, Giuseppe Pesce, Alejandro V Arzola, et al. Optical tweezers—from calibration to applications: a tutorial. Advances in Optics and Photonics, 13(1):74–241, 2021.

[6] Philip Jones, Onofrio Maragó, and Giovanni Volpe. Optical tweezers. Cambridge University Press Cambridge, 2015.

[7] Hu Zhang and Kuo-Kang Liu. Optical tweezers for single cells. Journal of the Royal Society interface, 5(24):671–690, 2008.

[8] Carlos Bustamante, Lisa Alexander, Kevin Maciuba, and Christian M Kaiser. Single-molecule studies of protein folding with optical tweezers. Annual Review of Biochemistry, 89(1):443–470, 2020.

[9] Carlos J Bustamante, Yann R Chemla, Shixin Liu, and Michelle D Wang. Optical tweezers in single-molecule biophysics. Nature Reviews Methods Primers, 1(1):25, 2021.

[10] The Nobel Prize. The nobel prize in physics 2018. https://www.nobelprize.org/prizes/physics/2018/ashkin/facts/, 2018. Accessed: 2025-05-04.

[11] James Clerk Maxwell. Viii. a dynamical theory of the electromagnetic field. Philosophical Transactions of the Royal Society of London, (155):459–512, 1865.

[12] John Henry Poynting. Xv. on the transfer of energy in the electromagnetic field. Philosophical Transactions of the Royal Society of London, (175):343–361, 1884.

[13] Arthur Ashkin. Acceleration and trapping of particles by radiation pressure. Physical Review Letters, 24(4):156, 1970.

[14] Arthur Ashkin, James M Dziedzic, John E Bjorkholm, and Steven Chu. Observation of a single-beam gradient force optical trap for dielectric particles. Optics Letters, 11(5):288–290, 1986.

[15] Arthur Ashkin. Optical trapping and manipulation of neutral particles using lasers. Proceedings of the National Academy of Sciences, 94(10):4853–4860, 1997.

[16] Keir C Neuman and Steven M Block. Optical trapping. Review of Scientific Instruments, 75(9):2787–2809, 2004.

[17] Miles Padgett and Richard Bowman. Tweezers with a twist. Nature Photonics, 5(6):343–348, 2011.

[18] Erwin JG Peterman, Frederick Gittes, and Christoph F Schmidt. Laser-induced heating in optical traps. Biophysical Journal, 84(2):1308–1316, 2003.

[19] Ann AM Bui, Anatolii V Kashchuk, Marie Anne Balanant, Timo A Nieminen, Halina Rubinsztein-Dunlop, and Alexander B Stilgoe. Calibration of force detection for arbitrarily shaped particles in optical tweezers. Scientific Reports, 8(1):10798, 2018.

[20] E Otte and C Denz. Optical trapping gets structure: Structured light for advanced optical manipulation. Applied Physics Reviews, 7(4), 2020.

[21] Kishan Dholakia and Tomáš Čižmár. Shaping the future of manipulation. Nature Photonics, 5(6):335–342, 2011.

[22] David McGloin. Optical tweezers: 20 years on. Philosophical Transactions of the Royal Society A: Mathematical, Physical and Engineering Sciences, 364(1849):3521–3537, 2006.

[23] Kevin D. Whitley, Matthew J. Comstock, and Yann R. Chemla. High-Resolution "Fleezers": Dual-Trap Optical Tweezers Combined with Single-Molecule Fluorescence Detection, pages 183–256. Springer New York, New York, NY, 2017.

[24] Giuseppe Pesce, Philip H Jones, Onofrio M Maragò, and Giovanni Volpe. Optical tweezers: theory and practice. The European Physical Journal Plus, 135:1–38, 2020.

[25] Alexander Rohrbach. Switching and measuring a force of 25 femtonewtons with an optical trap. Optics Express, 13(24):9695–9701, 2005.

[26] Andrea Gambassi and S Dietrich. Critical casimir forces in soft matter. Soft Matter, 20(15):3212–3242, 2024.

[27] Laura Pérez García, Jaime Donlucas Pérez, Giorgio Volpe, Alejandro V. Arzola, and Giovanni Volpe. High-performance reconstruction of microscopic force fields from brownian trajectories. Nature Communications, 9(1):5166, 2018.

[28] George Gabriel Stokes. On the effect of the internal friction of fluids on the motion of pendulums. 1851.

[29] Steven B Smith, Laura Finzi, and Carlos Bustamante. Direct mechanical measurements of the elasticity of single dna molecules by using magnetic beads. Science, 258(5085):1122–1126, 1992.

[30] Laura Pérez-García, Martin Selin, Antonio Ciarlo, Alessandro Magazzù, Giuseppe Pesce, Antonio Sasso, Giovanni Volpe, Isaac Pérez Castillo, and Alejandro V Arzola. Optimal calibration of optical tweezers with arbitrary integration time and sampling frequencies: a general framework. Biomedical Optics Express, 14(12):6442–6469, 2023.

[31] Raghuveer Parthasarathy. Rapid, accurate particle tracking by calculation of radial symmetry centers. Nature Methods, 9(7):724–726, 2012.

[32] Hui-Jun Cheng, Ching-Hsien Hsu, Che-Lun Hung, and Chun-Yuan Lin. A review for cell and particle tracking on microscopy images using algorithms and deep learning technologies. Biomedical Journal, 45(3):465–471, 2022.

[33] Saga Helgadottir, Aykut Argun, and Giovanni Volpe. Digital video microscopy enhanced by deep learning. Optica, 6(4):506–513, 2019.

[34] Weijie Tang, Ruohan Zhou, and Sheng Hu. A review of digital image processing techniques for optical tweezers: from algorithms to applications. Journal of Modern Optics, pages 1–16, 2025.

[35] Ian Goodfellow, Yoshua Bengio, Aaron Courville, and Yoshua Bengio. Deep learning, volume 1. MIT press Cambridge, 2016.

[36] Matthew D Zeiler and Rob Fergus. Visualizing and understanding convolutional networks. In European Conference on Computer Vision, pages 818–833. Springer, 2014.

[37] Alex Krizhevsky, Ilya Sutskever, and Geoffrey E Hinton. Imagenet classification with deep convolutional neural networks. Advances in Neural Information Processing Systems, 25, 2012.

[38] DeepTrackAI Team. Deeptrack 2.0. `https://github.com/deepTrackAI/deeptrack2`, 2025.

[39] Reza Azad, Ehsan Khodapanah Aghdam, Amelie Rauland, Yiwei Jia, Atlas Haddadi Avval, Afshin Bozorgpour, Sanaz Karimijafarbigloo, Joseph Paul Cohen, Ehsan Adeli, and Dorit Merhof. Medical image segmentation review: The success of u-net. IEEE Transactions on Pattern Analysis and Machine Intelligence, 2024.

[40] Olaf Ronneberger, Philipp Fischer, and Thomas Brox. U-net: Convolutional networks for biomedical image segmentation. In Medical image computing and computer-assisted intervention–MICCAI 2015: 18th international conference, Munich, Germany, October 5-9, 2015, proceedings, part III 18, pages 234–241. Springer, 2015.

[41] Nahian Siddique, Sidike Paheding, Colin P. Elkin, and Vijay Devabhaktuni. U-net and its variants for medical image segmentation: A review of theory and applications. IEEE Access, 9:82031–82057, 2021.

[42] Joseph Redmon, Santosh Divvala, Ross Girshick, and Ali Farhadi. You only look once: Unified, real-time object detection. In Proceedings of the IEEE Conference on Computer Vision and Pattern Recognition (CVPR), June 2016.

[43] Ravpreet Kaur and Sarbjeet Singh. A comprehensive review of object detection with deep learning. Digital Signal Processing, 132:103812, 2023.

[44] Glenn Jocher. Ultralytics yolov5, 2020.

[45] Keir C Neuman and Attila Nagy. Single-molecule force spectroscopy: optical tweezers, magnetic tweezers and atomic force microscopy. Nature Methods, 5(6):491–505, 2008.

[46] Xinming Zhang, Lu Ma, and Yongli Zhang. High-resolution optical tweezers for single-molecule manipulation. The Yale Journal of Biology and Medicine, 86(3):367, 2013.

[47] Carlos Bustamante, Jan Liphardt, and Felix Ritort. The nonequilibrium thermodynamics of small systems. Physics Today, 58(7):43–48, 2005.

[48] Steven B Smith, Yujia Cui, and Carlos Bustamante. Overstretching b-dna: The elastic response of individual double-stranded and single-stranded dna molecules. Science, 271(5250):795–799, 1996.

[49] Iddo Heller, Tjalle P Hoekstra, Graeme A King, Erwin JG Peterman, and Gijs JL Wuite. Optical tweezers analysis of dna–protein complexes. Chemical Reviews, 114(6):3087–3119, 2014.

[50] Claude Bouchiat, Michelle D Wang, J-F Allemand, T Strick, SM Block, and Vincent Croquette. Estimating the persistence length of a worm-like chain molecule from force-extension measurements. Biophysical Journal, 76(1):409–413, 1999.

[51] John F Marko and Eric D Siggia. Stretching dna. Macromolecules, 28(26):8759–8770, 1995.

[52] Michelle D Wang, Hong Yin, Robert Landick, Jeff Gelles, and Steven M Block. Stretching dna with optical tweezers. Biophysical Journal, 72(3):1335–1346, 1997.

[53] Annamaria Zaltron, Michele Merano, Giampaolo Mistura, Cinzia Sada, and Flavio Seno. Optical tweezers in single-molecule experiments. The European Physical Journal Plus, 135(11):896, 2020.

[54] Matthew TJ Halma, Jack A Tuszynski, and Gijs JL Wuite. Optical tweezers for drug discovery. Drug Discovery Today, 28(1):103443, 2023.

[55] Steven M Block, Lawrence SB Goldstein, and Bruce J Schnapp. Bead movement by single kinesin molecules studied with optical tweezers. Nature, 348(6299):348–352, 1990.

[56] Karel Svoboda, Christoph F Schmidt, Bruce J Schnapp, and Steven M Block. Direct observation of kinesin stepping by optical trapping interferometry. Nature, 365(6448):721–727, 1993.

[57] Elio A Abbondanzieri, William J Greenleaf, Joshua W Shaevitz, Robert Landick, and Steven M Block. Direct observation of base-pair stepping by rna polymerase. Nature, 438(7067):460–465, 2005.

[58] Hong Yin, Michelle D Wang, Karel Svoboda, Robert Landick, Steven M Block, and Jeff Gelles. Transcription against an applied force. Science, 270(5242):1653–1657, 1995.

[59] Rodrigo A Maillard, Gheorghe Chistol, Maya Sen, Maurizio Righini, Jiongyi Tan, Christian M Kaiser, Courtney Hodges, Andreas Martin, and Carlos Bustamante. Clpx(p) generates mechanical force to unfold and translocate its protein substrates. Cell, 145(3):459–469, 2011.

[60] Shixin Liu, Gheorghe Chistol, Craig L Hetherington, Sara Tafoya, K Aathavan, Joerg Schnitzbauer, Shelley Grimes, Paul J Jardine, and Carlos Bustamante. A viral packaging motor varies its dna rotation and step size to preserve subunit coordination as the capsid fills. Cell, 157(3):702–713, 2014.

[61] Jeffrey T Finer, Robert M Simmons, and James A Spudich. Single myosin molecule mechanics: piconewton forces and nanometre steps. Nature, 368(6467):113–119, 1994.

[62] Kerstin Ramser and Dag Hanstorp. Optical manipulation for single-cell studies. Journal of Biophotonics, 3(4):187–206, 2010.

[63] Haoqing Wang, Yuze Guo, Ran Zou, Huiqian Hu, Yao Wang, Fan Wang, and Lining Arnold Ju. Recent advances of optical tweezers–based dynamic force spectroscopy and mechanical measurement assays for live-cell mechanobiology. Frontiers in Physics, 10:771111, 2022.

[64] Ruixue Zhu, Tatiana Avsievich, Alexey Popov, and Igor Meglinski. Optical tweezers in studies of red blood cells. Cells, 9(3):545, 2020.

[65] Jochen Guck, Revathi Ananthakrishnan, Hamid Mahmood, Tess J Moon, C Casey Cunningham, and Josef Käs. The optical stretcher: A novel laser tool to micromanipulate cells. Biophysical Journal, 81(2):767–784, 2001.

[66] Marta Gironella-Torrent, Giulia Bergamaschi, Raya Sorkin, Gijs JL Wuite, and Felix Ritort. Viscoelastic phenotyping of red blood cells. Biophysical Journal, 123(7):770–781, 2024.

[67] Tuna Pesen, Bora Akgun, and Mehmet Burcin Unlu. Measuring the effect of repetitive stretching on the deformability of human red blood cells using optical tweezers. Scientific Reports, 15(1):9060, 2025.

[68] Jochen Guck, Stefan Schinkinger, Bryan Lincoln, Falk Wottawah, Susanne Ebert, Maren Romeyke, Dominik Lenz, Harold M Erickson, Revathi Ananthakrishnan, Daniel Mitchell, et al. Optical deformability as an inherent cell marker for testing malignant transformation and metastatic competence. Biophysical Journal, 88(5):3689–3698, 2005.

[69] Leonor Morgado, Estibaliz Gómez-de Mariscal, Hannah S Heil, and Ricardo Henriques. The rise of data-driven microscopy powered by machine learning. Journal of Microscopy, 295(2):85–92, 2024.

[70] David G Grier. Optical tweezers in colloid and interface science. Current Opinion in Colloid & Interface Science, 2(3):264–270, 1997.

[71] Duncan J. Shaw. 8 - colloid stability. In Duncan J. Shaw, editor, Introduction to Colloid and Surface Chemistry (Fourth Edition), pages 210–243. Butterworth-Heinemann, Oxford, fourth edition edition, 1992.

[72] Donald H Napper. Steric stabilization. Journal of Colloid and Interface Science, 58(2):390–407, 1977.

[73] Hendrick BG Casimir. On the attraction between two perfectly conducting plates. In Proc. Kon. Ned. Akad. Wet., volume 51, page 793, 1948.

[74] Andrea Gambassi. The casimir effect: From quantum to critical fluctuations. In Journal of Physics: Conference Series, volume 161, page 012037. IOP Publishing, 2009.

[75] Christopher Hertlein, Laurent Helden, Andrea Gambassi, Siegfried Dietrich, and Clemens Bechinger. Direct measurement of critical casimir forces. Nature, 451(7175):172–175, 2008.

[76] Sathyanarayana Paladugu, Agnese Callegari, Yazgan Tuna, Lukas Barth, Siegfried Dietrich, Andrea Gambassi, and Giovanni Volpe. Nonadditivity of critical casimir forces. Nature Communications, 7(1):11403, 2016.

[77] Svetoslav E Anachkov, Ivan Lesov, Michele Zanini, Peter A Kralchevsky, Nikolai D Denkov, and Lucio Isa. Particle detachment from fluid interfaces: theory vs. experiments. Soft Matter, 12(36):7632–7643, 2016.

[78] Anna Wang, Ryan McGorty, David M Kaz, and Vinothan N Manoharan. Contact-line pinning controls how quickly colloidal particles equilibrate with liquid interfaces. Soft Matter, 12(43):8958–8967, 2016.

[79] David M Kaz, Ryan McGorty, Madhav Mani, Michael P Brenner, and Vinothan N Manoharan. Physical ageing of the contact line on colloidal particles at liquid interfaces. Nature Materials, 11(2):138–142, 2012.

[80] Jacopo Vialetto, Michele Zanini, and Lucio Isa. Attachment and detachment of particles to and from fluid interfaces. Current Opinion in Colloid & Interface Science, 58(101560), 2022.

[81] Koen Visscher, Mark J Schnitzer, and Steven M Block. Single kinesin molecules studied with a molecular force clamp. Nature, 400(6740):184–189, 1999.

[82] Anna Alemany, Alessandro Mossa, Ivan Junier, and Felix Ritort. Experimental free-energy measurements of kinetic molecular states using fluctuation theorems. Nature Physics, 8(9):688–694, 2012.

[83] Joan Camunas-Soler, Anna Alemany, and Felix Ritort. Experimental measurement of binding energy, selectivity, and allostery using fluctuation theorems. Science, 355(6323):412–415, 2017.

[84] Alessandro Mossa, Sara de Lorenzo, Josep Maria Huguet, and Felix Ritort. Measurement of work in single-molecule pulling experiments. The Journal of Chemical Physics, 130(23), 2009.

[85] Anna Wypijewska del Nogal, Vinoth Sundar Rajan, Fredrik Westerlund, and L Marcus Wilhelmsson. Complex conformational dynamics of the heart failure-associated pre-mirna-377 hairpin revealed by single-molecule optical tweezers. International Journal of Molecular Sciences, 22(16):9008, 2021.

[86] Vinoth Sundar Rajan, Anna Wypijewska Del Nogal, Sune Levin, L Marcus Wilhelmsson, and Fredrik Westerlund. Exploring the conformational dynamics of the sars-cov-2 sl4 hairpin by combining optical tweezers and base analogues. Nanoscale, 16(2):752–764, 2024.

[87] Marc Rico-Pasto, Isabel Pastor, and Felix Ritort. Force feedback effects on single molecule hopping and pulling experiments. The Journal of Chemical Physics, 148(12), 2018.

[88] Giovanni Volpe Martin Selin, Antonio Ciarlo. Smarttrap repository. `https://github.com/softmatterlab/SmartTrap`, 2025. Accessed: 2025-08-08.

[89] Ognyan Moore, Nathan Jessurun, Martin Chase, Nils Nemitz, and Luke Campagnola. Pyqtgraph - high performance visualization for all platforms. In Proc. 22nd Python in Science Conference, pages 106–113, 2023.

[90] Hanchen Wang, Tianfan Fu, Yuanqi Du, Wenhao Gao, Kexin Huang, Ziming Liu, Payal Chandak, Shengchao Liu, Peter Van Katwyk, Andreea Deac, et al. Scientific discovery in the age of artificial intelligence. Nature, 620(7972):47–60, 2023.

[91] Daniil A Boiko, Robert MacKnight, Ben Kline, and Gabe Gomes. Autonomous chemical research with large language models. Nature, 624(7992):570–578, 2023.

[92] David Adam. The automated lab of tomorrow. Proceedings of the National Academy of Sciences, 121(17):e2406320121, 2024.

[93] Steven Euijong Whang, Yuji Roh, Hwanjun Song, and Jae-Gil Lee. Data collection and quality challenges in deep learning: A data-centric ai perspective. The VLDB Journal, 32(4):791–813, 2023.

[94] John Jumper, Richard Evans, Alexander Pritzel, Tim Green, Michael Figurnov, Olaf Ronneberger, Kathryn Tunyasuvunakool, Russ Bates, Augustin Žídek, Anna Potapenko, et al. Highly accurate protein structure prediction with alphafold. Nature, 596(7873):583–589, 2021.

[95] Monya Baker. 1,500 scientists lift the lid on reproducibility, 2016.

[96] Ian Holland and Jamie A Davies. Automation in the life science research laboratory. Frontiers in Bioengineering and Biotechnology, 8:571777, 2020.

[97] Matthew Praeger, Yunhui Xie, James A Grant-Jacob, Robert W Eason, and Ben Mills. Playing optical tweezers with deep reinforcement learning: in virtual, physical and augmented environments. Machine Learning: Science and Technology, 2(3):035024, 2021.

[98] Meng Yang, Yuzhi Shi, Qinghua Song, Zeyong Wei, Xiong Dun, Zhiming Wang, Zhanshan Wang, Cheng-Wei Qiu, Hui Zhang, and Xinbin Cheng. Optical sorting: past, present and future. Light: Science & Applications, 14(1):103, 2025.

[99] Xiaolin Wang, Shuxun Chen, Marco Kong, Zuankai Wang, Kevin D Costa, Ronald A Li, and Dong Sun. Enhanced cell sorting and manipulation with combined optical tweezer and microfluidic chip technologies. Lab on a Chip, 11(21):3656–3662, 2011.

[100] Kaidi Wang, Xiangyun Ma, Pierre-Luc Longchamps, Keng C Chou, and Xiaonan Lu. Single-cell identification and characterization of viable but nonculturable campylobacter jejuni using raman optical tweezers and machine learning. Analytical Chemistry, 97(4):2028–2035, 2025.

[101] Weijie Tang, Ruohan Zhou, and Sheng Hu. Dynamic detecting and particle counting of pearl chain in optical tweezers using deep learning approach. Optics Communications, page 132022, 2025.

[102] Matthew Peters, Sina Halvaei, Tianyu Zhao, Annie Yang-Schulz, Karla C Williams, and Reuven Gordon. Classification of single extracellular vesicles in a double nanohole optical tweezer for cancer detection. Journal of Physics: Photonics, 6(3):035017, 2024.

[103] Samira Chizari, Miles P Lim, Lucas A Shaw, Sydney P Austin, and Jonathan B Hopkins. Automated optical-tweezers assembly of engineered microgranular crystals. Small, 16(25):2000314, 2020.

[104] Jeffrey E Melzer and Euan McLeod. Assembly of multicomponent structures from hundreds of micron-scale building blocks using optical tweezers. Microsystems & Nanoengineering, 7(1):45, 2021.

[105] Peter E Hart, Nils J Nilsson, and Bertram Raphael. A formal basis for the heuristic determination of minimum cost paths. IEEE transactions on Systems Science and Cybernetics, 4(2):100–107, 1968.

[106] Karl Johan Åström and Tore Hägglund. Advanced PID control. ISA-The Instrumentation, Systems and Automation Society, 2006.

[107] Vincent François-Lavet, Peter Henderson, Riashat Islam, Marc G Bellemare, Joelle Pineau, et al. An introduction to deep reinforcement learning. Foundations and Trends® in Machine Learning, 11(3-4):219–354, 2018.

[108] Guanzhi Wang, Yuqi Xie, Yunfan Jiang, Ajay Mandlekar, Chaowei Xiao, Yuke Zhu, Linxi Fan, and Anima Anandkumar. Voyager: An open-ended embodied agent with large language models. arXiv preprint arXiv:2305.16291, 2023.

[109] Oriol Vinyals, Igor Babuschkin, Wojciech M Czarnecki, Michaël Mathieu, Andrew Dudzik, Junyoung Chung, David H Choi, Richard Powell, Timo Ewalds, Petko Georgiev, et al. Grandmaster level in starcraft ii using multi-agent reinforcement learning. Nature, 575(7782):350–354, 2019.